KEM-24: Effect of pressure maintenance by fluid injection on seismic hazard, Hazard analysis

Report | KEM-24 Report C

172147-REP01-FNV_SHA_KEM24 03 | Fugro NL Land B.V.

Document Control

Document Information

Project Title	KEM-24 "Effect of pressure maintenance by fluid injection on seismic hazard"
Document Title	KEM-24: Effect of pressure maintenance by fluid injection on seismic hazard, Hazard analysis
Fugro Project No.	172147
Fugro Document No.	172147-REP01-FNV_SHA_KEM24
Issue Number	03
Issue Status	Final Report
Fugro Legal Entity	Fugro France SAS
Issuing Office Address	115 Avenue de la Capelado, 34160 CASTRIES - France

Client Information

Client	Client: Ministry of Economic Affairs and Climate Policy
Client Address	Procurement Office, P.O. Box 93144, 2509 AC THE HAGUE

Revision History

Issue	Date	Status	Comments on Content	Prepared By	Checked By	Approved By
01	15 November 2021	For Review	Awaiting client comments	MLA, JMA, CDU, RSE	BWH	RSE
02	20 May 2022	For Review	Awaiting client comments	MLA, JMA, CDU, RSE	BWH	RSE
03	30 Sep 2022	Final		MLA, JMA, CDU, RSE	BWH	RSE

Project Team

Initials	Name	Role
CDU	Cedric DUVAIL	Senior Geologist, Project Manager
MLA	Manel LABIDI	Geologist
JMA	Judith MARINIERE	Seismologist
RSE	Ramon SECANELL	Senior Seismologist
BWH	Beau WHITNEY	Senior Geologist

Executive Summary

Fugro conducted an induced seismic hazard assessment of the Groningen gas field (Figure 1.1) taking into account the intermediate results of Dynafrax UG report for KEM-24 on the *effect of pressure maintenance by fluid injection on seismic risk.*

The goal was to establish, using synthetic seismic catalogs generated by Dynafrax using different injection gas hypothesis, which final fluid injection scenarios should be considered for the purposes of reservoir pressure maintenance and lowering the seismic risk profile.

Two site-specific probabilistic seismic hazard analyses (PSHA) were performed, using a methodology consistent with current international practice for industrial facilities and in agreement with EC8 recommendations. One PSHA considering only seismotectonic sources and one including induced seismic sources.

The hazard model used includes:

- Two (2) seismotectonic models;
- Five (5) Ground-Motion Prediction Equations (GMPEs);

The soil conditions considered correspond to standard rock with a V_{S30} = 200 m/s, which correspond to generic soil conditions in the Netherlands, where the standard rock conditions (Vs30=800 m/s) are not usual and soft soil conditions are often found.

Note that the calculations in this report are based on an existing probabilistic model (catalogue and seismotectonic models) used for an Offshore Windfarm project, in Netherlands, report P904711/SHA 01 (FUGRO, 2020). The regional model used corresponds to that probabilistic model and then, we included the induced seismicity produced by the different injection scenarios considered.

We considered the 4 different scenarios provided by Dynafrax (arbitrary hypothetical scenarios selected), associated with different injection rates. The four scenarios considered (see Figure 6.1) were:

- Scenario 1: 60 years of depletion from 1960 to 2020, 10 years of injection (up to 2030) and 20 years of shut-in (up to 2050)
- Scenario 2: 60 years of depletion from 1960 to 2020, 1 years of injection (up to 2022) and 29 years of shut-in (up to 2050)
- Scenario 3: 60 years of depletion from 1960 to 2020, 30 years without activity (called reference period), 10 years of injection (up to 2060) and 20 years of shut-in (up to 2080)
- Scenario 3: 60 years of depletion from 1960 to 2020, 30 years without activity (called reference period), 5 years of injection (up to 2055) and 25 years of shut-in (up to 2080)

For each one of these scenarios and for two periods of time (injection time only or injection with a shut-in period), a seismic occurrence distribution (Gutenberg-Richter law) was determined and the seismic hazard, taking into account the new induced zone (corresponding to Groningen reservoir) in the seismotectonic model and its seismic occurrence distribution, was estimated.

Conclusion on induced seismicity

Independently of the scenario used, the seismic occurrence distribution of the induced zone (Groningen reservoir) showed higher seismic activity levels than the natural seismotectonic zone if we consider a period equivalent to the injection time only. This means that the seismic activity rate ($\lambda_{ind}(M)/km^2$ value) of the induced zone is always higher than the seismic activity rate ($\lambda_{nat}(M)/km^2$) of the natural seismotectonic zone where Groningen is situated. However, we note that the natural seismic activity of the Groningen region is very low. So that even a low induced seismicity contribution can become significant compared to the background seismic activity. We should also note that if we consider a longer period of 30 years (such as injection time + shut-in), scenarios 1, 2 and 4 will have similar seismic activity levels than the natural seismotectonic zone.

As a result of that, considering a period equivalent to the injection time only, we found that the introduction of the induced seismicity in the seismic hazard model, independently of the scenario, increases in a non-negligible way the seismic hazard of the Groningen region. However, we note that:

1) Despite the non-negligible increase in the seismic hazard, it remains very low, less than 0.04 g for the worst case scenario at 475 years return period. However, we have to note that the consideration of a 475 years return period assumes the hypothesis of stationarity along the time, which would be a very conservative hypothesis. This value is significantly lower than the PGA predicted in past TNO report, where the PGA was fixed at 0.117g (see chapter 2.5). Very likely the reason is the low seismic activity predicted by the modelling used here, compared with the really observed seismicity used in TNO report (see chapter 2.5)

2) The injection induced change in seismic hazard should only occur for the 1, 5 or 10 years of injection simulation. After these 1, 5 or 10 years (depending on the scenario chosen) the seismic hazard returns to its natural baseline, without any induced seismicity consideration (with mean PGA around 0.015 g).

3) The induced seismicity only produces small earthquakes (the M_{max}<4.0 based on the simulations performed) and the associated seismic accelerations from these events would be lower than 0.1 g, except in extreme cases (i.e., considering the median acceleration predicted by the GMPE plus 3 standard deviations).

4) When the injection of fluid is stopped, the simulations indicate that the induced seismicity diminishes to close to zero.

5) Based on the seismic hazard associated to each scenario, the best scenario would be to follow the procedure of Scenario 1 (considering an injection period of 10 years) that leads to an increase of only 30 % at 475 years return period and can even be reduced to 11 % considering a period of 30 years (injection time + shut-in). The increase of seismic activity rates would be lower with longer periods of time. In any case, the introduction of injection increases the seismic hazard for the 4 scenarios tested.

Therefore, we can conclude that, from the seismic hazard point of view the “best action” for induced seismicity is to allow the system to re-equilibrate pressures in a natural way. The injection of fluids, considering several different scenarios tested, leads to an increase in the seismicity rate and, therefore, to an increase of the seismic hazard. This increase is temporal being controlled by the injection duration and affects predominantly small ground accelerations.

Contents

1. Introduction

Fugro conducted an induced seismic hazard and risk assessment for the Groningen gas field (Figure 1.1) following the induced seismic scenarios defined by Dynafrax UG for the KEM-24 project. The scenarios tested were defined to test the effect of pressure maintenance by fluid injection on seismic risk.

The goal was to establish, using numerical/synthetic seismicity catalogues generated by Dynafrax, the effect on seismic hazard of several fluid injection scenarios. To achieve this, a PSHA was performed that considered natural and induced seismic sources. For the PSHA, one calculation point was used for simplicity and comparison purposes. It corresponds to the central point of the Groningen reservoir, close to the city of Loppersum.

Coordinates of the calculation point used for the PSHA are specified in Table 1.1.

Table 1.1: Coordinates of the calculation point for the PSHA.

Coordinates (WGS 84)	
Latitude (°)	Longitude (°)
53.328367°N	6.762381°E

The Groningen gas field (GGF) is located in an area of very low natural seismic activity according to GSHAP seismic hazard maps (Giardini *et al.*, 1999), with Peak Ground Acceleration (PGA) values below 0.2 m/s^2, for rock conditions at the 475-year return period. The area of interest is far from moderate natural seismic sources of the Netherlands which are situated in the south of country in the Roer Valley Graben (Limburg area).

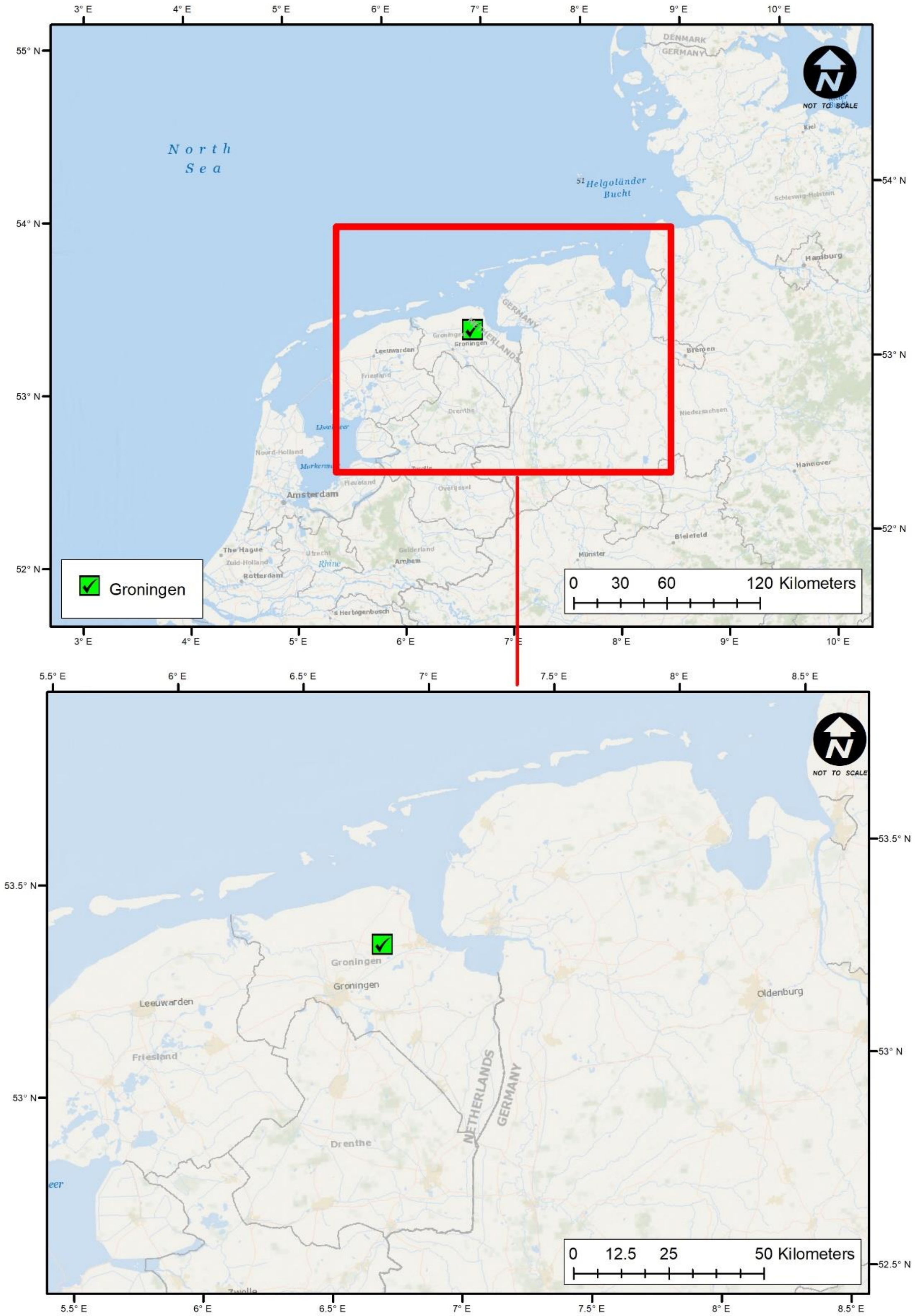

Figure 1.1: Location of the Groningen gas field.

1.1 Scope and purpose

The objective of this study was the evaluation of induced seismicity using modelling of different injection scenarios to determine its influence on the seismic hazard of the region.

To perform this evaluation, we performed 2 different calculations:

1) A seismic hazard assessment taking into account only natural seismotectonic sources
2) A seismic hazard assessment taking into account the seismotectonic sources and the induced seismicity.

In this study, we were mainly interested in the comparison of these seismic hazard calculations. Typically, for regions where the seismic activity is very high (i.e., in Indonesia, Chile or other tectonically active areas), induced seismicity from human activities is negligible for the local seismic hazard because the relatively low magnitudes produced by induced sources are not significant compared to larger and more frequent natural seismic activity.

However, in zones with less natural seismicity, the consideration of induced seismic sources (i.e., case of Groningen) can produce a non-negligible increase to the seismic hazard.

For this study, firstly, a probabilistic seismic hazard assessment (PSHA) at the Groningen gas field that considers only natural seismicity was conducted. The probabilistic model used was defined in a PSHA performed by Fugro for an Offshore Windfarm project, in 2020.

Uncertainties related to the delineation of seismic sources and ground motion models are considered according to state-of-the-art methods and propagated in the probabilistic approach through logic trees**.**

Then, a second PSHA was the performed considering the previous probabilistic model (considering only natural seismotectonic seismicity) with the addition of a new induced seismic source associated with injection activities in the Groningen field.

The induced seismicity was assumed to occur at 3 km depth, equivalent to average Groningen reservoir depth. The V_{S30} value adopted was 200 m/s and one calculation point was considered at the center of the Groningen reservoir area, close to the city of Loppersum.

Then, we compared the ground motion values derived from each assessment. The comparison is done using seismic hazard curves (annual exceedance rates of different acceleration levels). Due to the time dependency (the injection will only happen for 10 years or less with shut-in periods from 20 to 29 years), we do not define response spectra associated with longer return periods.

We have to note that the seismic hazard assessment was performed using the current industrial practice for seismic hazard assessment of critical facilities. It means that the seismic activity rates are supposed to be stationary. However, we know that the induced seismicity is not stationary. To take into account the non-stationarity, some temporal slices were considered. In each slice, the induced seismicity is supposed to be stationary. Therefore, the seismic hazard assessment here presented should be considered as a first approximation of the reality. In Groningen, TNO developed more sophisticated probabilistic models using nonstationary models. However, at the time of the realization of this study the models were not public available and we decided the use of standard models for seismic hazard assessment.

We have to note also that the central part of the KEM-24 project was the development of fluid injection models and not a very detailed seismic hazard assessment (which was already performed in Groningen). The main objective was the comparison between the seismic hazard with and without consideration of the induced seismicity. To do this comparison, we used one of the output data of the fluid injection modelling: the induced seismic catalogues. Then, these seismic catalogues associated to different fluid injection scenarios were used to perform the seismic hazard assessment considering induced seismicity. Even if the seismic hazard assessment can be considered only as a first approximation to the reality, we consider that the seismic hazard assessment performed allows to identify if the fluid injection scenarios used could lead to significant increments (or not) of the seismic hazard. Therefore, the seismic hazard assessment results, even if they were defined using stationary models of seismicity, allow the identification of seismic hazard increments and facilitate further decisions by authorities.

1.2 Organisation of the report

The purpose of this report is to present the results of the probabilistic seismic hazard analyses and a comparison of their results. It is organized as follows:

- Chapter 2 concerns the review and evaluation of previous seismic hazard studies conducted by others in the region. It provides background information on the ground motion estimates of Groningen area and provides a means to compare the PSHA results obtained in this study. As the objective is the comparison between the seismic hazard with and without induced seismicity, the review of seismic hazard assessments considering only natural seismicity demonstrates the range of values (or uncertainty) achieved by others. This provides a frame of reference for the impact of including induced seismicity in the assessment;
- Chapter 3 describes the methodology for determining the seismic ground motions in both seismic hazard assessment performed (with and without induced sources);
- Chapter 4 presents the declustered earthquake catalogue used;
- Chapter 5 describes the alternative seismotectonic models used;
- Chapter 6 presents the methodology to derive:
    - the seismic activity parameters for all the zones of each seismotectonic model;
    - the seismic activity parameters of the induced zone;
- Chapter 7 presents the ground motion prediction equations (GMPEs) used in this study;
- Chapter 8 presents the description of the logic tree, global parameters for PSHA calculation and the computed ground motions for the natural and induced seismicity models;
- Chapter 9 provides the conclusions of this study;
- Chapter 10 includes the references used for the study.

2. Review of previous seismic hazard assessment studies

PSHA results, considering only natural seismicity, at the Groningen reservoir are quite similar for all of the publications analysed. The region where the gas field is situated corresponds to a low natural seismicity region, a so called "Stable Continental Region" (SCR) as opposed to "Active Crustal Region".

In terms of PGA, the results previously published generally range from 0.01 g (0.1 m/s^2) to 0.02 g (0.2 m/s^2), for rock conditions at a return period of 475 years and considering only natural seismicity.

2.1 Seismic zoning map conforming to Eurocode 8 for the Netherlands (Crook, 1996)

References:

CROOK, Th. de, (1996), A seismic zoning map conforming to Eurocode 8, and practical earthquake parameter relations for the Netherlands, *Geologie en Mijnbouw,* 75, pp 11-18.

BROUWER J.W.R. (2010). The meaning of Eurocode 8 and Induced Seismicity For Earthquake Engineering in the Netherlands. Fifth International Conference on Recent Advances in Geotechnical Earthquake Engineering and Soil Dynamics, May 24-29, 2010, San Diego, California.

De Crook (1996) performed the latest seismic hazard study for the Netherlands, considering natural seismicity, based on the earthquake catalogue up to 1993. Figure 2.1 and Figure 2.2 show the maps of seismic hazard zones in the Netherlands based on this study. These maps are used as the current hazard zonation map in the Netherlands. An update of this study using a revised and extended catalogue of earthquakes and new ground motion prediction relations is being prepared at the KNMI (Koninklijk Nederlands Meteorologisch Instituut). Ground motions are used instead of intensities, which is more convenient for engineering purposes and can be compared with actual measurements (Brouwer, 2010).

The seismic zonation map of the Netherlands is based on a seismic hazard study with a 10 % probability of exceedance in 50 years (return period of 475 years).

Four seismic zones are defined, where for stiff soil type, the PGAs are respectively:

- Seismic zone A: PGA = 0.10 m/s^2 (0.01 g);
- Seismic zone B: PGA = 0.22 m/s^2 (0.022 g);
- Seismic zone C: PGA = 0.50 m/s^2 (0.05 g);
- Seismic zone D: PGA = 1.00 m/s^2 (0.1 g).

On this seismic hazard map, the Groningen Gas Field is located in a region associated to an estimated **PGA value lower than 0.1 m/s^2 (zone A) along the northern coast of the Netherlands, at the return period of 475 years** (Figure 2.2). This seismic level corresponds to a very low seismic hazard.

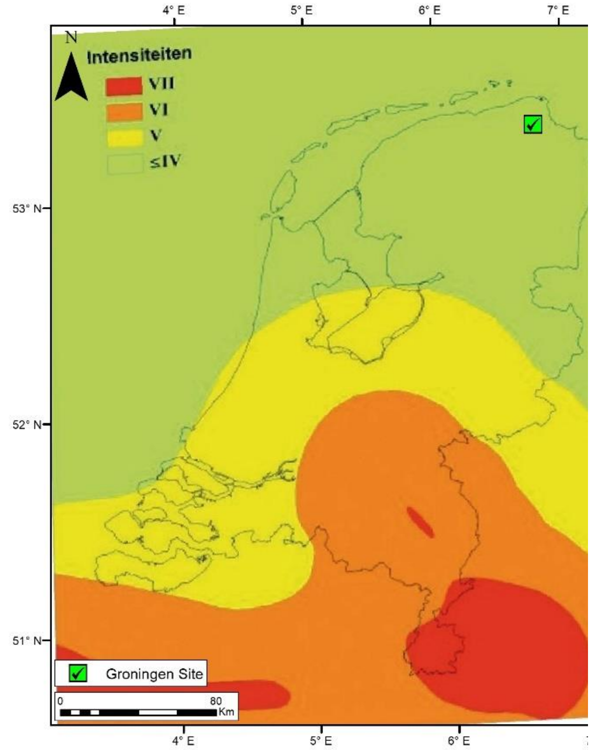

Figure 2.1: Currently available seismic hazard zonation in the Netherlands in terms of intensity (Crook, 1996).

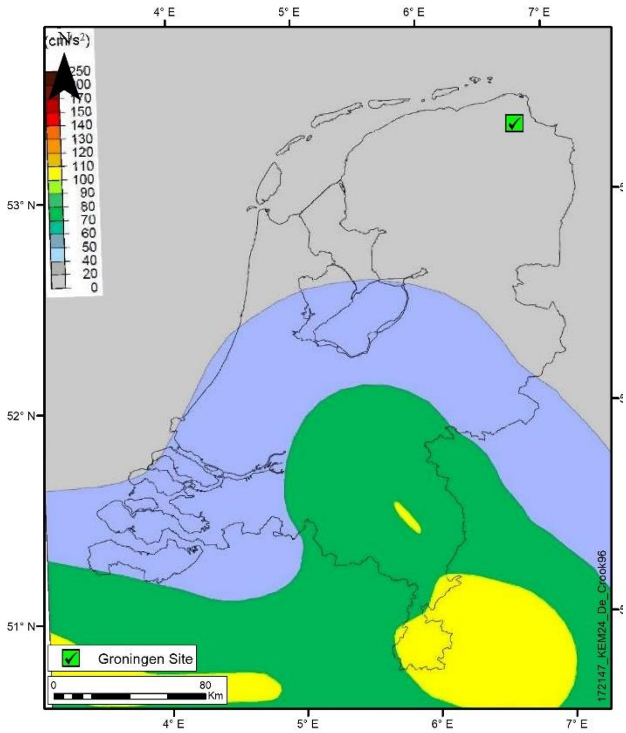

Figure 2.2: Seismic zonation map of the Netherlands based on a seismic hazard study with a 10% of exceedance in 50 years (return period 475 years).

2.2 Global Seismic Hazard Assessment Program

References:

GRÜNTHAL, G., BOSSE, C., SELLAMI, S., MAYER-ROSA, D. & GIARDINI, D. (1999). Compilation of the GSHAP regional seismic hazard for Europe, Africa and the Middle East. www.seismo.ethz.ch/static/GSHAP/index.html

A seismic hazard map was published by GSHAP (Global Seismic Hazard Assessment Program) for the region (Grünthal *et al.,* 1999). The objective of the GSHAP program was to propose a global seismic hazard map at the world scale, based on homogenized and coordinated probabilistic approach.

Figure 2.3 is an extract of the global GSHAP hazard map focusing on the project region. This map shows the PGA expected with 10% probability of exceedance in 50 years.

The area of interest of the Groningen Gas Field corresponds on the GSHAP map to a region where estimated **PGA values are below 0.2 m/s^2 along the northern coast of the Netherlands, at the return period of 475 years** (Figure 2.3). This seismic level corresponds to a very low seismic hazard, considering only natural seismicity.

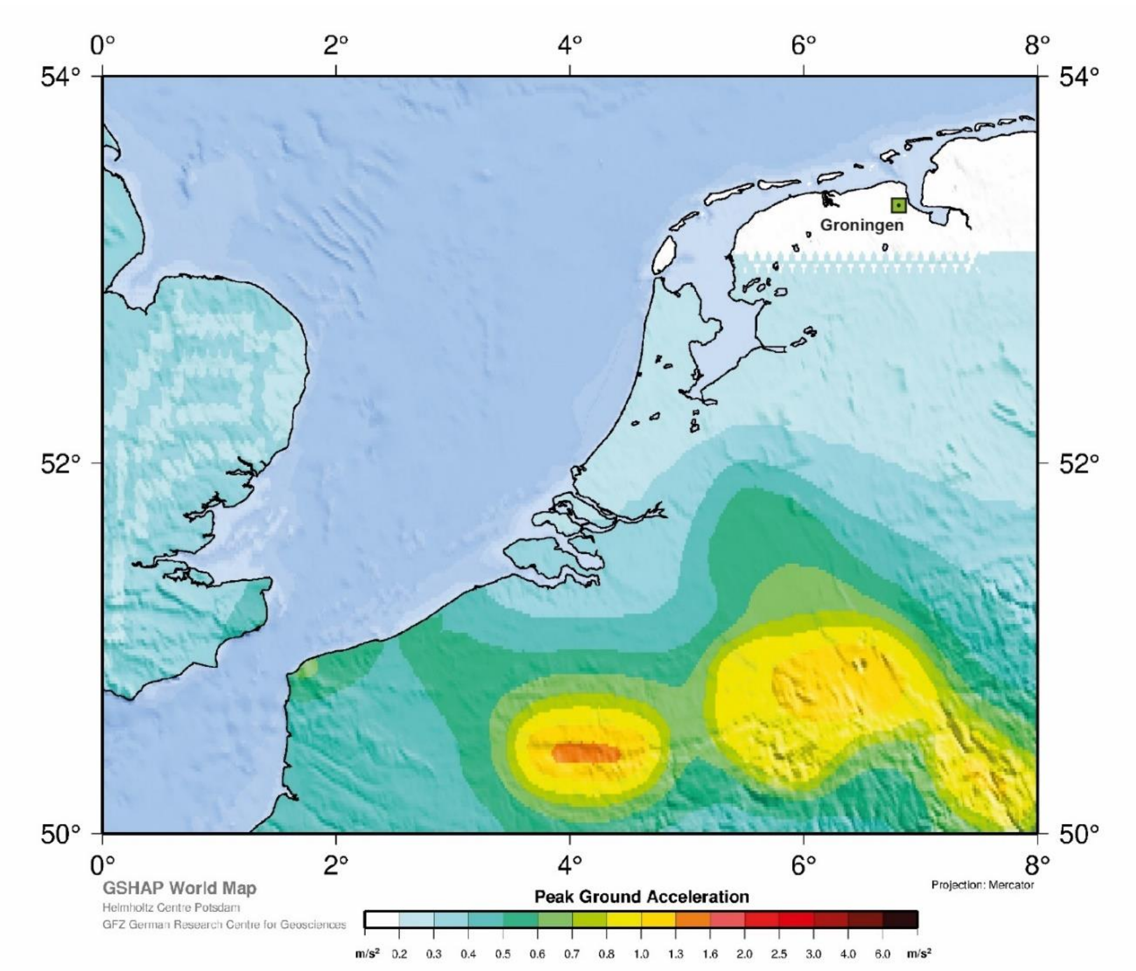

Figure 2.3: Seismic hazard map for a return period of 475 years according to GSHAP (Grünthal *et al.,* 1999) (data and plotting tool from http://gmo.gfz-Potsdam.de/) and location of the Groningen Gas Field.

2.3 The 2013 European Seismic Hazard Model: Key Components and Results (SHARE Project)

References:

GIARDINI, D., J. WOESSNER, L. DANCIU (2014) Mapping Europe's Seismic Hazard. EOS, 95(29): p. 261-262.

WOESSNER, J., DANCIU L., D. GIARDINI and the SHARE consortium (2015), The 2013 European Seismic Hazard Model: key components and results, *Bull. Earthq. Eng.*, doi:10.1007/s10518-015-9795-1.

The 2013 European Seismic Hazard Model (ESHM13) results from a community-based probabilistic seismic hazard assessment supported by the EU-FP7 project "Seismic Hazard Harmonization in Europe" (SHARE, 2009–2013). The ESHM13 is a consistent seismic hazard model for Europe and Turkey which overcomes the limitation of national borders and includes a thorough quantification of the uncertainties. It corresponds to the first completed regional effort contributing to the "Global Earthquake Model" initiative.

Seismic hazard calculations were computed for a standard rock condition (i.e., V_{S30}= 800 m/s, Pagani *et al.*, 2014). Several maps at different return periods (*i.e.*, 475, 975, 2 475 and 4 975 years) were produced.

In this publication, and at the return period of 475 years (10 % exceedance in 50 years), the PGA is lower than 0.01 g (0.1 m/s^2) along the northern coast of the Netherlands (Figure 2.4).

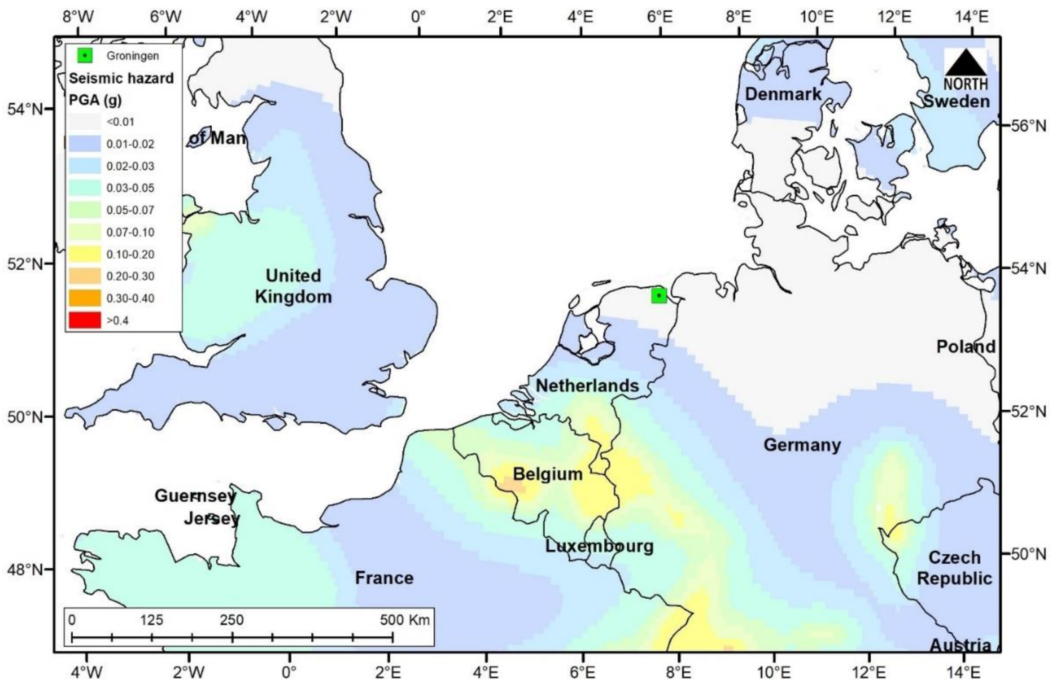

Figure 2.4: Extract from SHARE map showing the PGA at 475-year return period (10% chance of exceedance in 50 years) and location of the Groningen Gas Field.

2.4 Global Earthquake Model

References:

M. PAGANI, J. GARCIA-PELAEZ, R. GEE, K. JOHNSON, V. POGGI, R. STYRON, G. WEATHERILL, M. SIMIONATO, D. VIGANÒ, L. DANCIU, D. MONELLI (2018). Global Earthquake Model (GEM) Seismic Hazard Map (version 2018.1 - December 2018), DOI: 10.13117/GEM-GLOBAL-SEISMIC-HAZARD-MAP-2018.1

The Global Earthquake Model (GEM) is a non-profit foundation that works to develop and disseminate global earthquake hazard information to inform the public and policy makers. The most recent global seismic hazard map (version 2018.1) was created by collating and aggregating a global database of regional and national probabilistic seismic hazard models. These models are then used to calculate hazard values for the globe for reference rock conditions (V_{S30} of 760-800 m/s).

Similar to the GSHAP model, the GEM hazard map presents an overview of hazard variability at large scale.

In this publication, the PGA at the return period of 475 years is lower than 0.01 g (0.1 m/s²) along the northern coast of the Netherlands, which is consistent with a region of low seismicity (Figure 2.5).

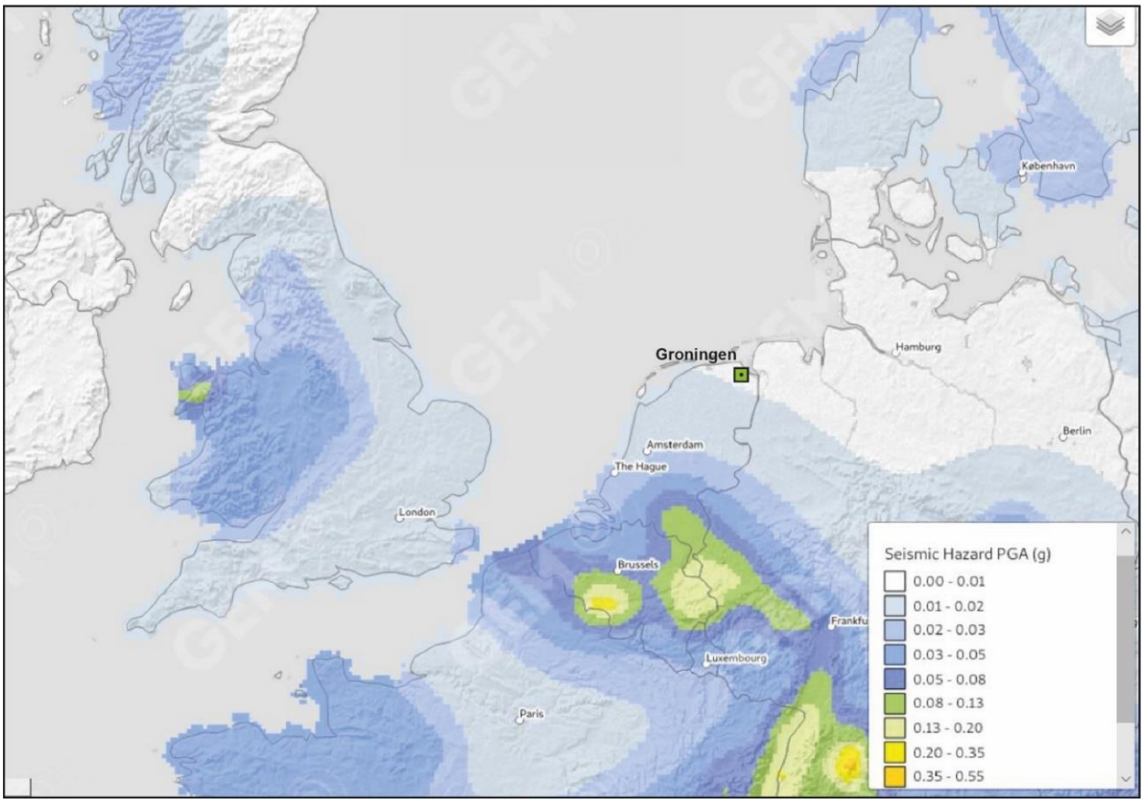

Figure 2.5: Extract from GEM 2018 showing the 10% chance of exceedance in 50 years (PGA) and location of the Groningen Gas Field.

2.5 TNO Model Chain

References:

J.J BOMMER, B. EDWARDS, P.P. KRUIVER, A. RODRIGUEZ-MAREK, P.J. STAFFORD, M. NTINALEXIS, E. RUIGROK, J. SPETZLER (2019). V6 Ground-Motion Model (GMM) for Induced Seismicity in the Groningen Field with Assurance Letter. NAM report.

TNO (2020a). Probabilistic Seismic Hazard and Risk Analysis in the TNO Model Chain Groningen, TNO 2020 R11052.

TNO (2020b). TNO Model Chain Groningen: Update and quick scan comparison of 2020 HRA model, TNO 2020 R11659.

TNO were commissioned by the Ministry of Economic Affairs and Climate of the Netherlands (EZK) to develop a probabilistic seismic hazard and risk assessment (PSHRA) procedure (i.e. a model chain) for application to target sites within the public domain surrounding and within the Groningen gas field. The TNO Model Chain was developed to replicate the hazard and risk assessment (HRA) models of the independent Groningen operator NAM using an independent software implementation. The seismic hazard component of the TNO Model Chain comprises of the seismic source model (SSM) and the ground motion model (GMM).

The SSM forecasts the temporal-spatial distribution of the gas depletion induced earthquakes and their magnitudes, conditional on the specified production scenario. The use of the SSM implicitly assumes that the Groningen seismicity is treated as non-stationary, reflecting the non-Poisson temporal distribution of these earthquakes due to resulting from gas depletion. Induced earthquakes in the Groningen gas field are assumed to be caused by differential compaction on existing faults.

The SSM uses static data such as reservoir geometry, reservoir compressibility and fault data to model the relationship between gas depletion, reservoir compaction and subsurface faulting. Historic induced earthquake and field pore pressure changes are required to train this compaction model to forecast future induced earthquakes. For a given gas production scenario, the compaction model computes vertical strains based on the associated pore pressure changes. These vertical strains are combined with the fault data to compute spatial and temporal distributions of Coulomb stress changes. Main shock seismicity distributions in time and space are then computed from the spatial and temporal distributions of Coulomb stress changes. The SSM implements an Epidemic-Type Aftershock Sequence (ETAS) model to compute aftershock seismicity distribution corresponding to the main shock seismicity distribution. The main shock and aftershock seismicity distributions are combined to provide a total seismicity distribution. A b-value is then assigned to these seismic events to define the Gutenberg-Richter magnitude distribution. The magnitude distribution is bounded by a maximum probable magnitude. The total seismicity distribution is now defined in time, space and magnitude. A rupture model then translates the generated hypocenter locations into rupture plane distributions with associated magnitudes. The final output of the SSM is therefore a statistical distribution of total seismicity of a specific magnitude, at a specific distance and within a specific year, for each point at the surface given a specific production scenario.

The TNO Model Chain GMM has recently been updated to implement GMM V6 of Bommer et al. (2019). Given a specific magnitude and rupture distance, the Bommer et al. (2019) GMM V6 provides statistical distributions of horizontal ground motions for 23 spectral periods, PGV and ground motion duration. Ground motions were computed for bedrock corresponding to the base of the North Sea Group at a depth of approximately 800 m. A site-response zonation model defined within Bommer et al. (2018) is used to translate the bedrock motions to the surface.

Within the seismic hazard component of the TNO Model Chain the SSM and GMM are convolved to produce the seismic hazard estimates for a given production scenario in the form of annual probabilities of exceedance for given intensities of spectral acceleration for each grid point at the surface. These results can be presented as hazard curves, or as hazard maps for a specific year following the onset of the production scenario. Hazard curves and hazard maps are computed for specific years rather than for specific return periods because non-stationary earthquakes are considered in the TNO Model Chain, rather than stationary earthquakes as within conventional PSHA.

The TNO Model Chain reports provide a hazard map for PGA (treated as equivalent to T = 0.01 s spectral accelerations) for the gas production year 2020/2021 assuming time zero at the beginning of 2020 (Figure 2.6). Then, using the induced seismicity predicted during the 2020/2021 period and assuming a return period of 475 years (implicitly, it means that a stationarity seismicity is considered), the maximum PGA computed for this production scenario (0.117 g) is stronger than our most conservative scenario (Scenario 2 with an injection period of 1 year) giving 0.04 g. We have to note that the TNO model forecasts 7.86 events of magnitude 1.5 or above for one year. This annual activity rate is higher than the annual activity rates predicted in any of the scenarios considered in this study.

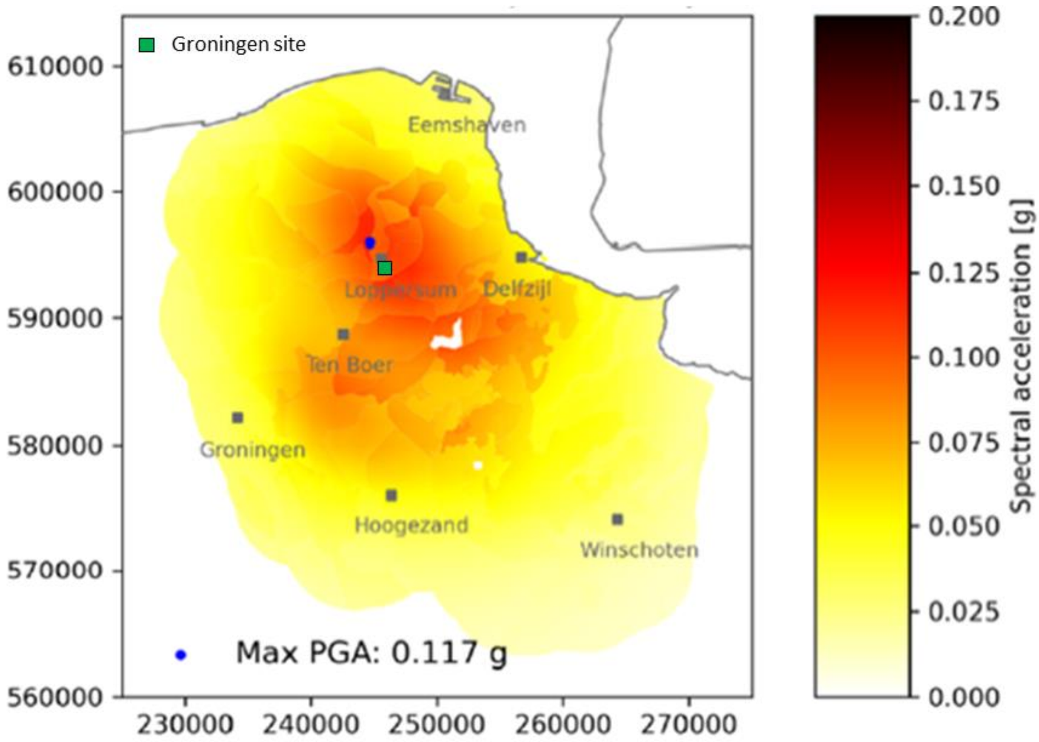

Figure 2.6: Extract from TNO (2020b) showing the PGA values in the Groningen field and the surrounding regions observed for the 2020/2021 gas production year.

3. Methodology

3.1 Methods for determining ground motions

Two methods are commonly applied in seismic hazard assessment studies: deterministic and probabilistic methods. These two approaches provide complementary results. The deterministic approach usually focuses on a single earthquake scenario, 'worst-case scenario', while the probabilistic approach combines all possible scenarios taking into account their probabilities of occurrence. The two approaches can lead to different results depending on the seismotectonic environment of the site of interest. International guidelines and standards nowadays recommend the probabilistic approach since it allows for a better treatment of the uncertainties. However, the deterministic approach is still used to complement the probabilistic results and is still the reference method in a couple of national regulations.

For this study, a probabilistic seismic hazard assessment has been conducted.

3.2 Probabilistic approach

The probabilistic method follows the traditional calculation process developed by Cornell (1968) (Figure 3.1). The basic assumptions are that the seismicity in a region can be modeled by a set of independent sources and a Poisson occurrence of events with time.

The estimated annual rate at which the ground motion, A, will exceed a particular value, a, is computed by (Cornell 1968):

$$\lambda[A > a] = \sum_{i=1}^{Nsource} N(M_{min}) \iint P[A > a|m,r]\, f_M(m)\, f_R(r)\, dm\, dr$$

where N_{source} is the total number of sources, $N(M_{min})$ is the annual rate of earthquakes with magnitude greater than or equal to M_{min}, $P[A > a|m,r]$ is the probability of the ground motion, A, exceeding the threshold value a, given the earthquake magnitude m and distance r from the source, and $f_M(m)$ and $f_R(r)$ are probability density functions describing magnitude and distance. Integration over all the magnitudes and distances is performed. The computation of this integral is carried out numerically. Under the Poissonian assumption, the probability of exceedance in a specified exposure period t (typically corresponding to the useful life of a project) $P[A > a,t]$ is related to the annual rate of exceedance $\lambda[A > a]$ by:

$$P[A > a,t] = 1 - e^{-[\lambda[A>a]\, t]}$$

In this study the seismic sources are modeled as area sources in which the probability of future earthquakes occurrence is homogeneous where no specific seismotectonic structures can be identified.

Then, the seismic activity was modeled using the well-known Gutenberg-Richter model.

The calculation process is based on a logic tree in order to propagate epistemic and aleatory uncertainties.

The PSHA was performed using the following steps:

- Compilation and processing of the earthquake catalogue (including declustering and definition of completeness periods for magnitude ranges);
- Identification and characterization of seismic sources of the seismotectonic models;
- Definition of the ground motion prediction equations (GMPEs, sometimes called 'attenuation laws');
- The construction of a logic tree based on the consideration of a set of alternative seismotectonic models and GMPEs;
- Hazard calculation results in a set of hazard curves (one for each branch of the logic-tree). A hazard curve gives the probabilities of exceedance at the site for given acceleration levels;

The software used to derive the seismicity parameters is the Fugro proprietary code GEOSIS (2018) developed by Fugro and, for seismic hazard calculations, a version of R-CRISIS specifically developed by Mario Ordaz *et al.* (2017) for Fugro. R-CRISIS is the newest version of CRISIS, a worldwide and well-known solution for performing PSHAs accounting for both aleatory and epistemic uncertainties using logic-tree computations. R-CRISIS has been verified and validated during the last PEER project "Probabilistic Seismic Hazard Analysis Code Verification" (Hale et al. 2018). The resulting hazard model will be the probabilistic combination of branches representing different assumptions and the weights assigned to them.

The PSHA is performed assuming soft soil conditions in terms of V_{S30} defined as representative of the Groningen Gas Field (V_{S30} = 200m/s).

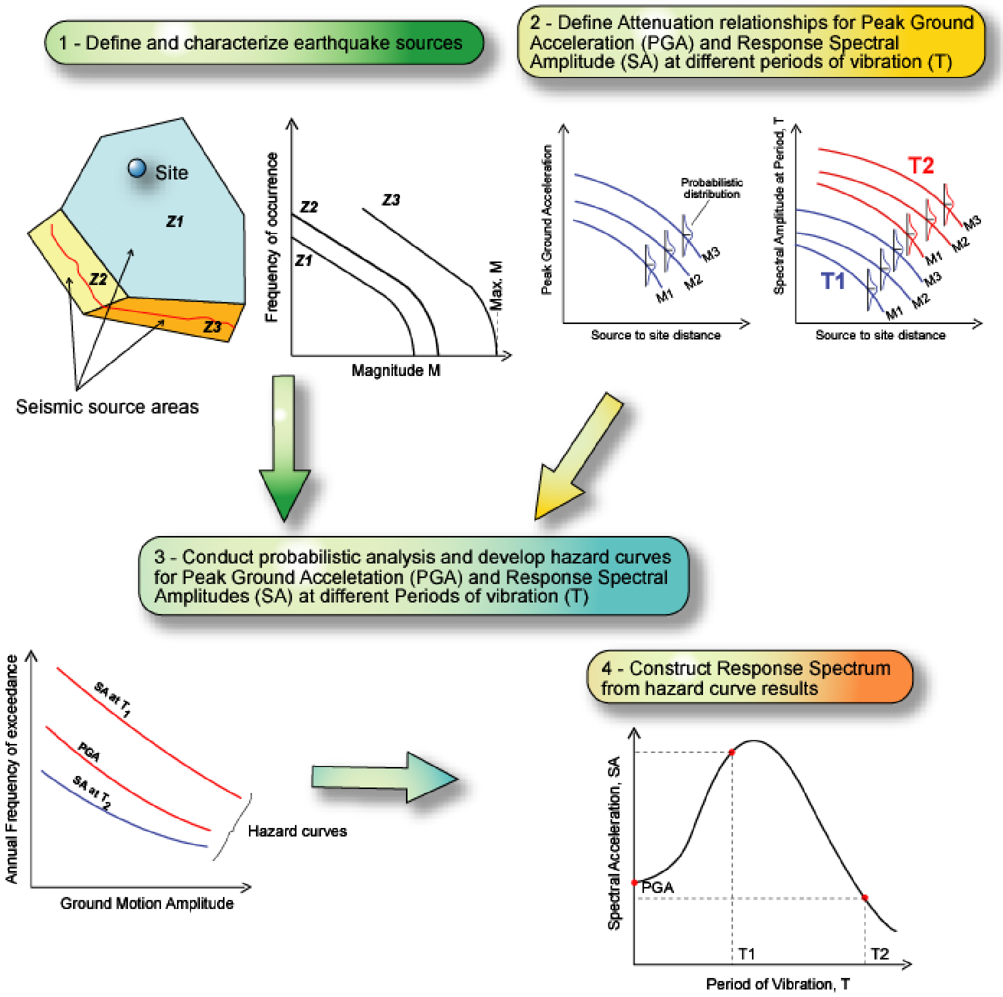

Figure 3.1: Probabilistic seismic hazard method flowchart.

4. Seismological database

The earthquake catalogue (seismotectonic origin) used in this study correspond to that defined for an Offshore Windfarm project (Fugro, 2020). Here below we only present only a summary of the characteristics of the seismic catalogue developed in that project.

For a detailed explanation on the seismological database, please refer to the previous work done for the Offshore Windfarm project, in the report P904711/SHA 01 (FUGRO, 2020).

The induced catalogue used is the synthetic seismicity catalogue provided by Dynafrax during this project considering 4 different injection scenarios. In PSHA calculations considering induced seismicity, the induced catalogue is "superposed" to the natural seismic catalogue.

4.1 Earthquake catalogue with seismotectonic origin

4.1.1 Data compilation

The earthquake catalogue covering the historical and instrumental periods was compiled for the study area from different sources and includes records spanning almost 640 years (from 1382 to 2019). Considering the tectonic setting and the seismicity around the study area, the compiled catalogue is made in a radius of 300 km around the site covering an area between 0° to 15°E of longitude and 48°N to 58°N of latitude.

The following databases were considered to develop the project catalogue:

- The International Seismological Centre (ISC) which is a global catalogue compiling information from various global and local networks. 19 195 events with reported magnitudes were compiled for the period from 1900 to 2019. (http://www.isc.ac.uk/iscbulletin/search/bulletin/).
- The Royal Netherlands Meteorological Institute (KNMI) catalogue provides information on date, hour, coordinates, depth, local magnitude and event type of each event. 1,408 events were compiled for the period from 1911 to 2019. (https://data.knmi.nl/datasets/aardbevingen_catalogus/1).
- The British Geological Survey (BGS) catalogue which provides information on recent and historical earthquakes. 11,595 events were compiled for the period from 1382 to 2019. (http://www.earthquakes.bgs.ac.uk/earthquakes/dataSearch.html).
- The Royal Observatory of Belgium (ROB) catalogue covers the period from 1382 to 2018 and includes 7 530 events. (http://seismologie.be/fr/seismologie/sismicite-en-belgique/banque-de-donnees-en-ligne).

The final compiled catalogue for this study, based on all catalogues mentioned above, contains 33 688 earthquakes, before duplicate removal, covering the period from 1382 to end of December 2019.

4.1.2 Final compiled declustered catalogue

After the removal of duplicate events, induced seismicity, the magnitude homogenization, we obtained a final processed catalogue with the following characteristics:

- 23,368 events
- Period 1382 – 2019
- 0.1 ≤ Mw ≤ 6.09
- 0 ≤ hypocentral depth ≤ 87.7 km

For the declustering, the Gardner & Knopoff (1974) algorithm was used, together with the space and time windows of Burkhard & Grünthal (2009),

The declustered catalogue is mapped on Figure 4.1.

4.1.3 Completeness analysis

In order to compute activity rates, one needs to estimate completeness periods which correspond to dates after which all events of a given magnitude range are detected and included in the seismicity catalogue.

The estimated completeness years for the different magnitude bins are given in Table 4.1, including best-estimate, lower and upper bounds to consider uncertainty on these estimations.

Table 4.1: Completeness period (best-estimates, lower and upper bounds) by magnitude bins for the project catalogue.

Mw	Best estimate	Lower Bound	Upper Bound
[1.5 – 2.0)	1990	1980	2000
[2.0 – 2.5)	1980	1965	1995
[2.5 – 3.0)	1975	1960	1990
[3.0 – 3.5)	1970	1950	1985
[3.5 – 4.0)	1950	1920	1980
[4.0 – 4.5)	1900	1850	1950
[4.5 – 5.0)	1850	1800	1900
≥ 5.0	1800	1700	1900

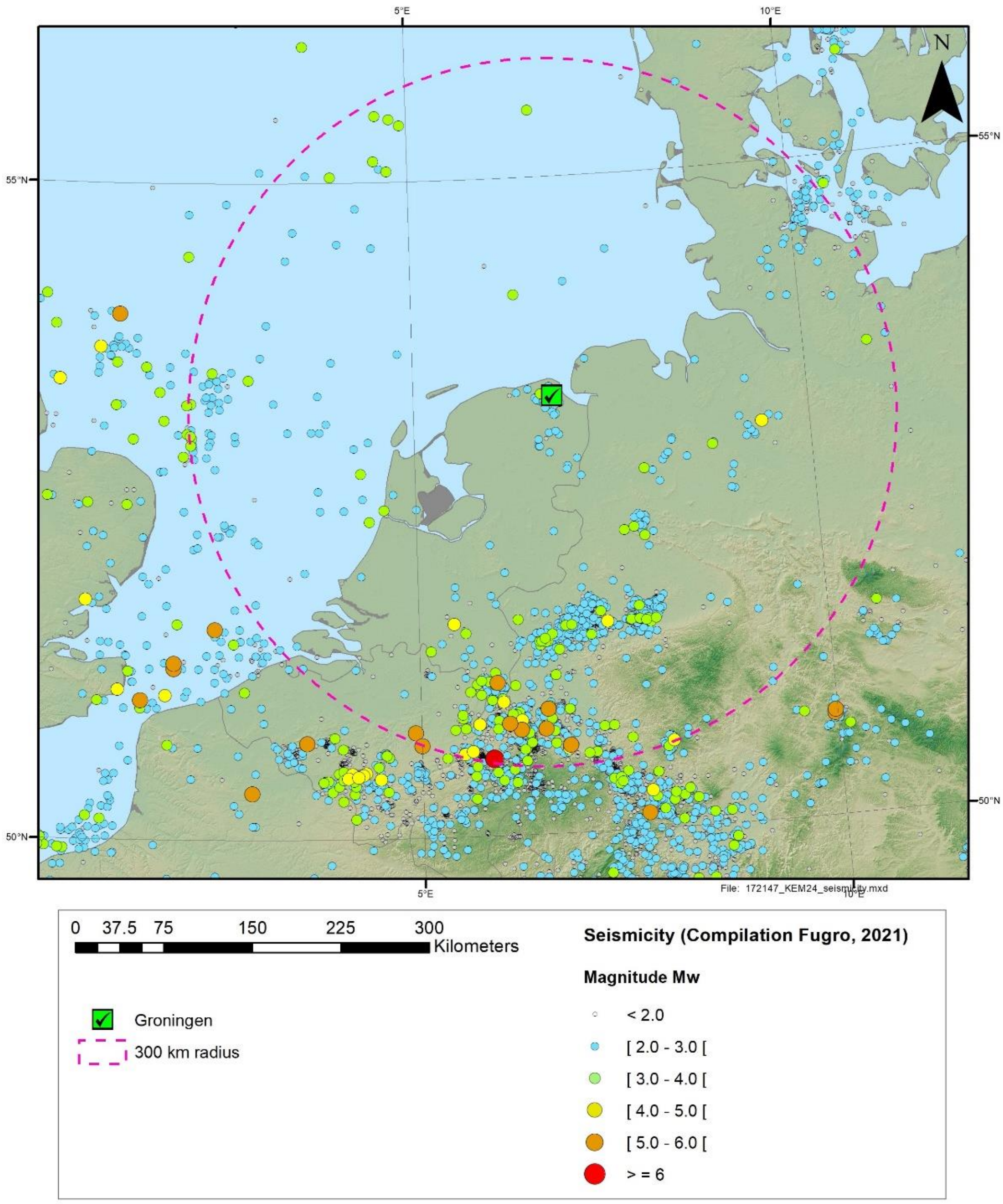

Figure 4.1: Seismicity of the region of interest (period 1352 to 2019) – Declustered catalogue.

4.2 Induced earthquake catalogue

The seismicity catalogues considered are presented in the Table 4.2, Table 4.3, Table 4.4 and Table 4.5 and Figure 4.2, Figure 4.3, Figure 4.4 and Figure 4.5 and they were provided by Dynafrax (see Figure 6.1). The different injection scenarios (see Figure 6.1) are also shown in Figure 4.2, Figure 4.3, Figure 4.4 and Figure 4.5.

Table 4.2: Seismic catalogue associated to Scenario 1 (source: Dynafrax)

ID	Longitude	Latitude	Magnitude	Occurrence date
1	6.6309	53.2955	1.93	2021.03.18
2	6.7568	53.2354	2.22	2021.07.07
3	6.8761	53.2655	2.44	2021.07.16
4	6.8259	53.2838	2.39	2024.04.28

Table 4.3: Seismic catalogue associated to Scenario 2 (source: Dynafrax)

ID	Longitude	Latitude	Magnitude	Occurrence date
1	6.8761	53.2655	2.45	2021.01.24
2	6.7568	53.2354	2.21	2021.02.04
3	6.6309	53.2955	1.93	2021.03.19
4	6.8664	53.1973	1.45	2021.06.09
5	6.8259	53.2838	2.39	2021.06.24
6	6.8397	53.2734	1.48	2021.10.02
7	6.8828	53.2934	2.01	2021.10.18
8	6.8528	53.2531	1.96	2021.12.21
9	6.8615	53.2792	2.02	2021.12.28

Table 4.4: Seismic catalogue associated to Scenario 3 (source: Dynafrax)

ID	Longitude	Latitude	Magnitude	Occurrence date
1	6.8761	53.2655	2.43	2052.02.02
2	6.8259	53.2838	2.38	2053.02.26
3	6.5647	53.3013	2.20	2063.01.24

Table 4.5: Seismic catalogue associated to Scenario 4 (source: Dynafrax)

ID	Longitude	Latitude	Magnitude	Occurrence date
1	6.8761	53.2655	2.41	2051.03.19
2	6.8259	53.2838	2.38	2051.07.31
3	6.8664	53.1973	1.43	2052.01.11
4	6.8828	53.2934	1.99	2052.07.11
5	6.8397	53.2734	1.41	2053.07.26
6	6.8254	53.2106	2.18	2054.02.22
7	6.7070	53.2089	2.25	2054.07.03
8	6.8335	53.2273	1.47	2055.01.18
9	6.5647	53.3013	2.20	2055.02.05
10	6.8728	53.2199	1.99	2055.08.28
11	6.9440	53.2070	2.24	2055.11.04
12	6.8836	53.2887	2.15	2055.12.26
13	6.8490	53.2578	2.06	2056.01.10

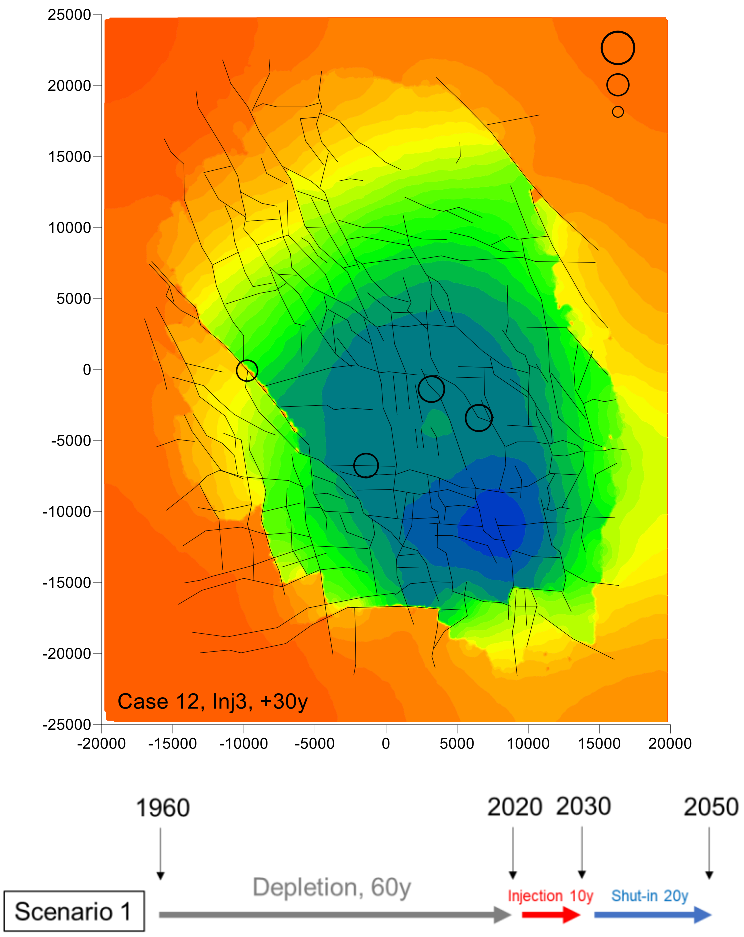

Figure 4.2: Seismic catalogue associated to Scenario 1 (source: Dynafrax).

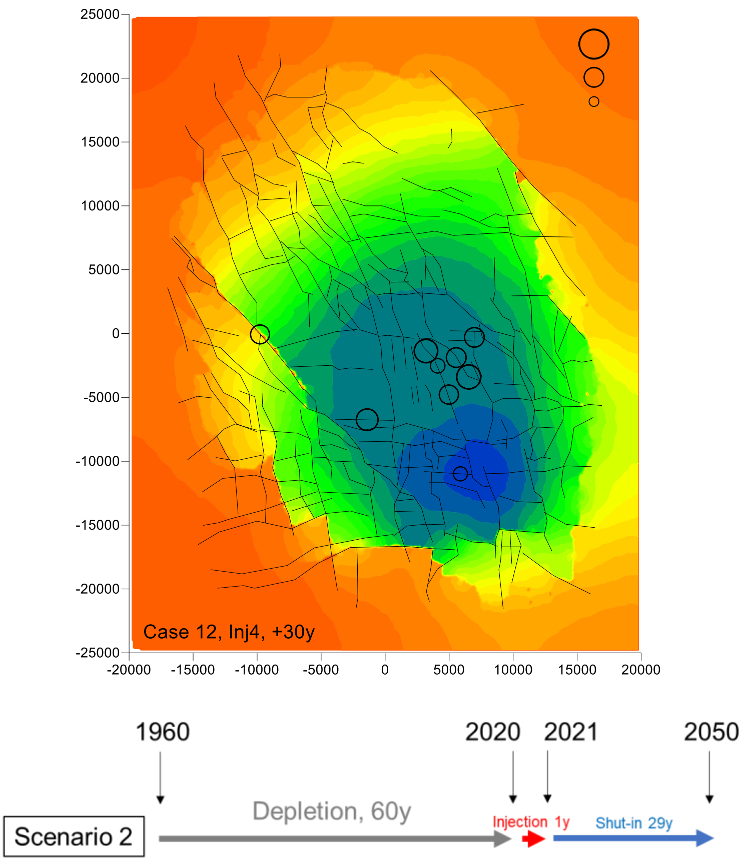

Figure 4.3: Seismic catalogue associated to Scenario 2 (source: Dynafrax).

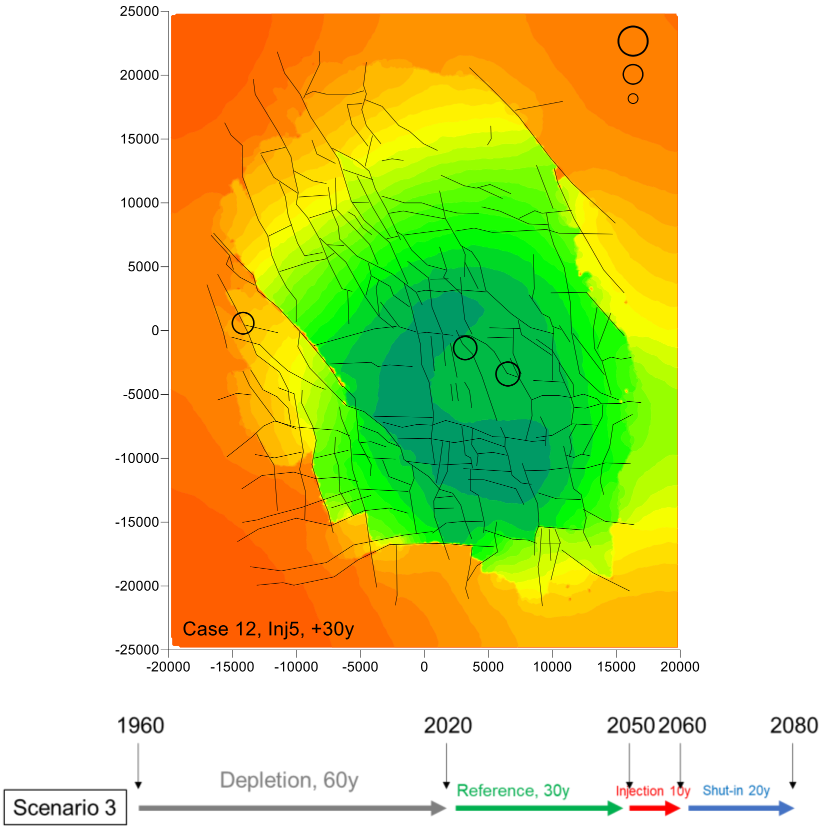

Figure 4.4: Seismic catalogue associated to Scenario 3 (source: Dynafrax).

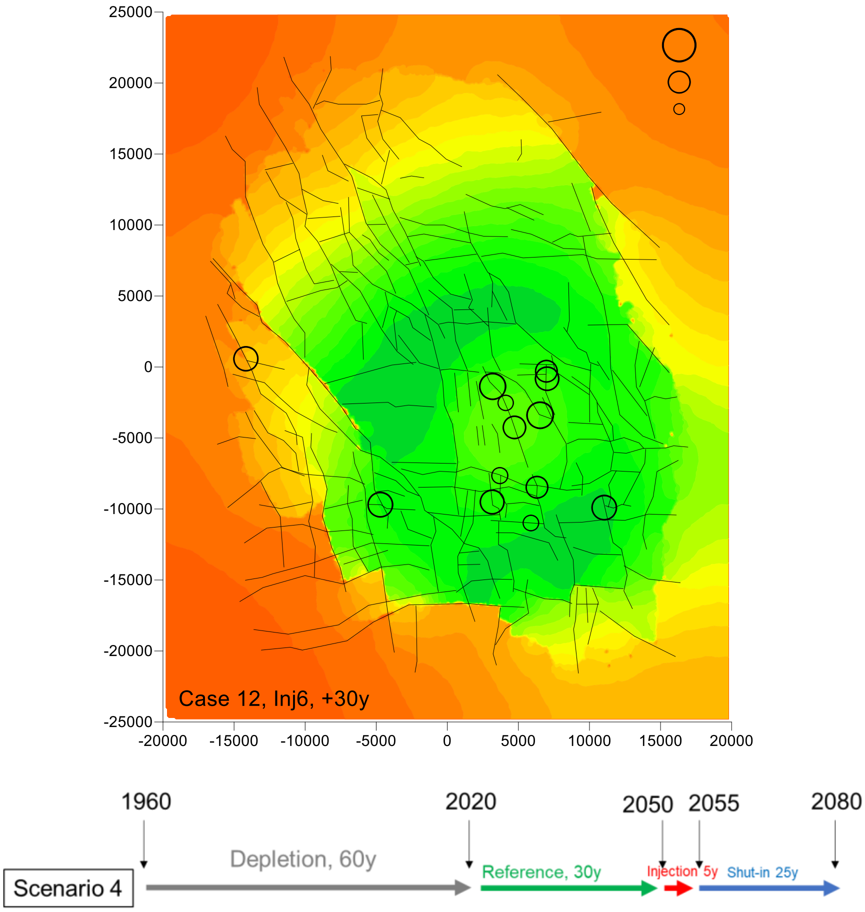

Figure 4.5: Seismic catalogue associated to Scenario 4 (source: Dynafrax).

5. Seismic sources

The seismotectonic models used in this study correspond to that defined for an Offshore Windfarm project. Below we present only a summary of the characteristics of the seismotectonic models developed in that project.

The development of seismotectonic models and the seismic source parameters are explained in detail in the FUGRO report P904711/SHA 01 (FUGRO, 2020).

5.1 Seismotectonic Model

Two seismotectonic models defined in a 300 km radius around the Groningen site were used:

- **Model 1 (M1)** is composed by 16 areal seismic sources (Figure 5.1). This model is mainly derived from the French seismotectonic zonation developed for probabilistic seismic hazard assessment for the French Metropolitan territory published by Le Dortz *et al.* (2019). The Groningen site is situated in WCB zone, which dominates the seismic hazard at the site.
- **Model 2 (M2)** is composed by 17 areal seismic sources (Figure 5.2). The model is mainly based on the seismic model published by Verbeek et al. (2009) for Belgium. Groningen site is situated in zone 20, which dominates the seismic hazard at the site.

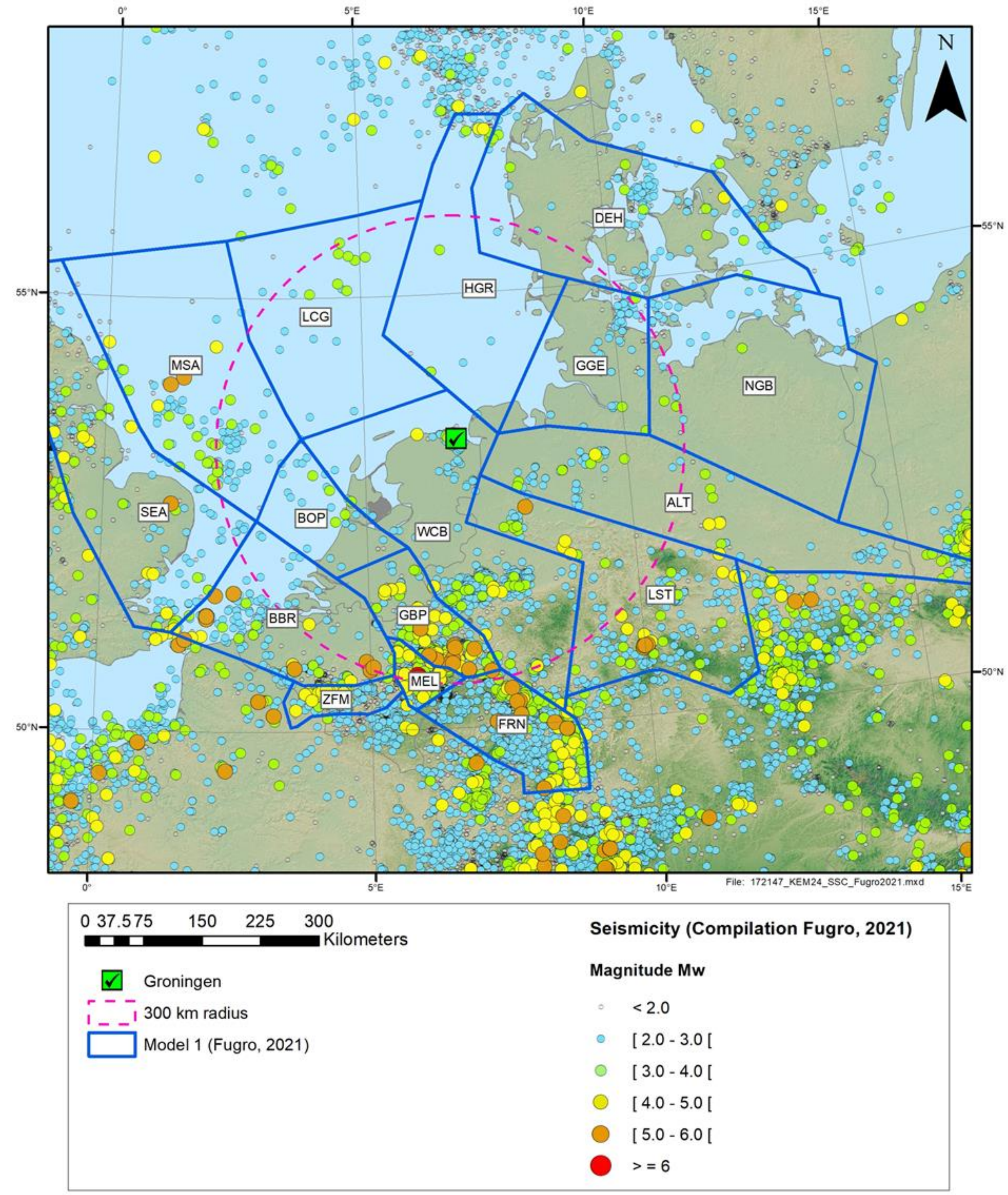

Figure 5.1: Seismotectonic model developed by Fugro (2021), modified from Le Dortz *et al.*, 2019 for the Groningen site – Model 1.

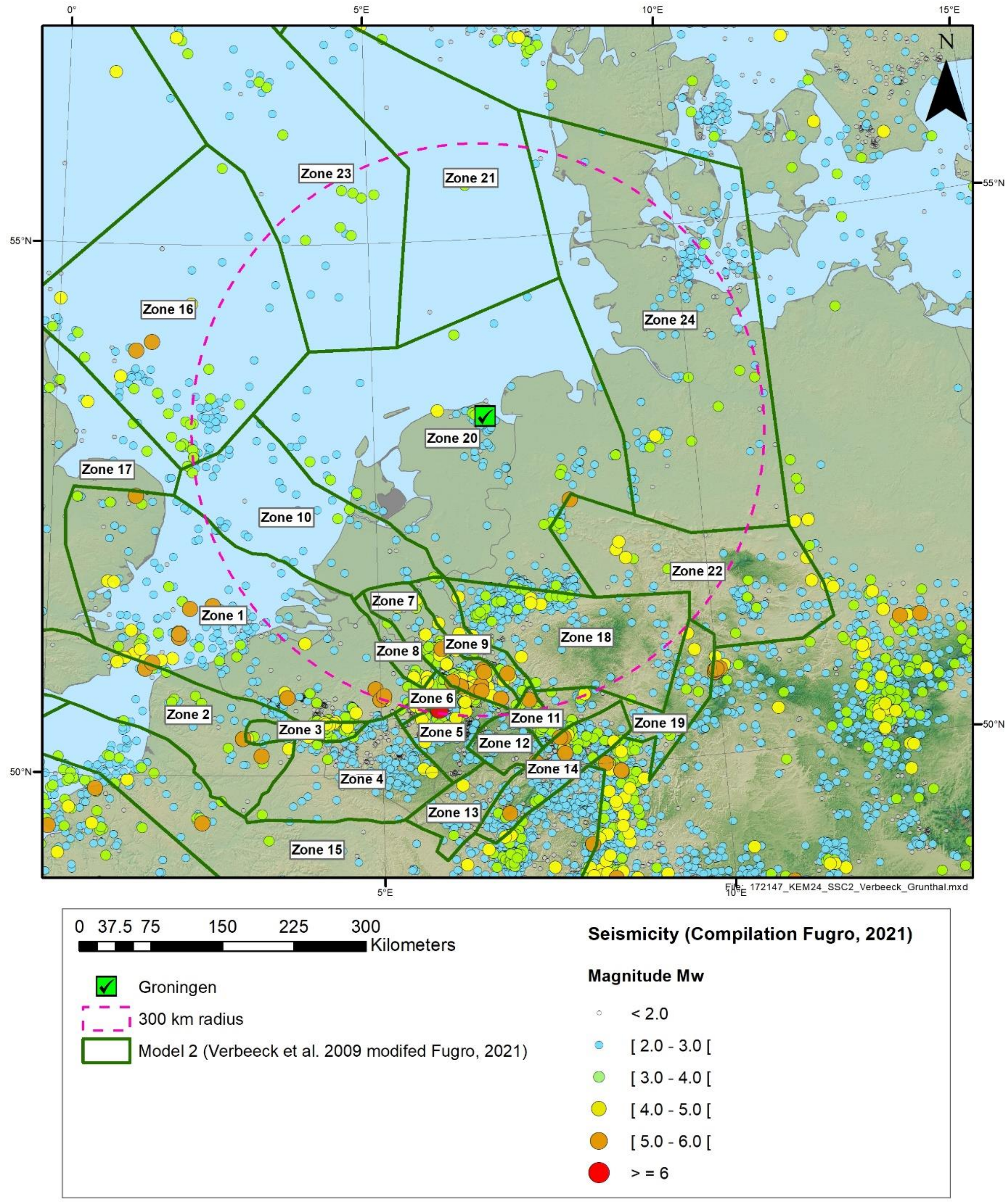

Figure 5.2: Seismotectonic model 2 used of the Groningen site (After Verbeek *et al.,* 2009, modified Fugro, 2021).

5.2 Induced Model

In the Groningen Gas Field, we define the model as an area of 1216 km^2 (thick black line on Figure 5.3) representative of the oval shape of the reservoir (grey area on Figure 5.3), from the report of Dynafrax UG. The depth considered for the occurrence of earthquakes was 3 km.

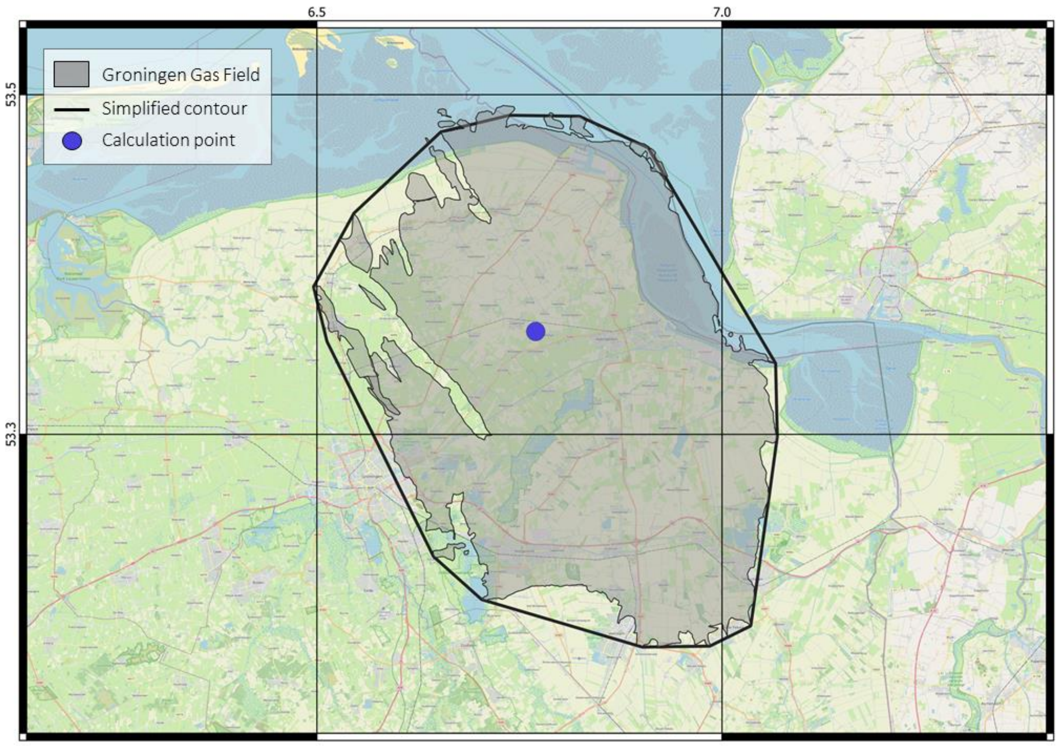

Figure 5.3: Area chosen (thick black line) to represent the Groningen Gas Field (grey area) used for the seismic source model.

6. Seismic activity model

6.1 Presentation

For the natural seismotectonic sources, the computation of seismic activity rates is based on the Gutenberg-Richter (GR) model, assuming stationary seismic rates (a declustered catalogue was used for PSHA calculations). The TNO Model Chain was not publicly available at the time of redaction of this report. A classical approach using stationary models is used which is common in international practice.

The method used to determine the coefficients *a* and *b* of the model is based on the EPRI (2012) method which is an updated and improved version of the Weichert (1980) method. In particular, it allows:

- The consideration of non-uniform magnitude bins;
- The use of regionally varying completeness periods;
- The introduction of a prior on the slope of the GR model (b-value).

The regional completeness is accounted for directly in the calculation. Each zone of the seismotectonic models can overlap with multiple zones of completeness, in which case the observed activity rates are computed counting the number of events in each sub-zone and taking into account the corresponding completeness periods. It is useful for seismotectonic models with significant regional variation of completeness periods. However, for this study, the regional variation of completeness was not found to be significant. Hence the single set of completeness periods is sufficient for all the zones of the seismotectonic models considered.

The fit is performed if at least two magnitude bins are populated (implying at least two events with different magnitudes). Otherwise, the b-value is fixed at the prior value and only the a-value is estimated.

The prior b-value is set to 1.0 in this study.

For the induced sources, the hypothesis is to use a stationary model that will only be valid for a specific period of time (injection time only or injection time + shut-in) to simulate the non-stationarity of the induced model. The results will be expressed in terms of annual exceedance rate for a specific time window.

The process used to define the GR law of the induced source is presented in Chapter 6.2.3.

In PSHA calculations using R-CRISIS (2019), the assignment of the seismic parameters for each areal source is based on parameters λ and β which essentially corresponds to a-value and b-value respectively following the minimum magnitude considered for PSHA calculations. Here, we used M_{min}=2.0 for the induced seismicity model and M_{min}=3.5 for the seismotectonic model to take into account the low magnitudes associated with induced seismicity.

6.2 Gutenberg-Richter definition

6.2.1 Seismotectonic Model 1

The classical Gutenberg-Richter (GR) fit parameters (a and b-value of the typical GR laws, annual activity rate of the Poisson distribution considered, λ, and β value of the exponential distribution assumed for magnitudes, and their associated errors) for all the zones associated to seismotectonic Model 1 are shown in Table 6.1.

6.2.2 Seismotectonic Model 2

The GR fit parameters (a, b, λ, β and associated errors) for all the zones associated to seismotectonic Model 2 (Verbeeck, 2009; modified Fugro, 2020) are shown in Table 6.2.

Table 6.1: Gutenberg-Richter parameters for Model 1 (modified FUGRO, 2020)

Zone	M_{min} (fit)	a (normalized to 10^6 km^2)	a (scaled to area of zone)	σa	b	σb	λ (M_{min}=3.5)	σ λ (M_{min}=3.5)	β	σ β
BBR	2.0	3.6975	2.2219	0.0468	0.9642	0.0763	0.0704	0.0076	2.2201	0.1757
BOP	J94*	3.4582	1.7210	0.0300	0.9750	0.0470	0.0203	0.0048	2.2450	0.1082
EBP	3.5	3.8148	2.6586	0.1773	1.0946	0.1767	0.0672	0.0275	2.5203	0.4069
FRN	1.5	4.3774	2.6669	0.0170	0.9298	0.0288	0.2586	0.0101	2.1410	0.0662
GBP	2.0	4.2801	2.3412	0.0371	0.9248	0.0590	0.1272	0.0109	2.1294	0.1359
GEM	1.5	2.9631	1.6229	0.0450	0.8090	0.0604	0.0619	0.0064	1.8628	0.1391
HGR	2.0	2.8720	1.5272	0.1086	0.9812	0.1398	0.0124	0.0031	2.2593	0.3218
LCG	3.0	3.8728	2.5698	0.1448	1.1322	0.1650	0.0405	0.0135	2.6069	0.3798
LSH	2.0	3.8831	2.2527	0.0678	1.1341	0.1205	0.0192	0.0030	2.6113	0.2774
MCE	2.0	3.3646	2.0472	0.0523	0.9266	0.0799	0.0637	0.0077	2.1335	0.1839
MEL	2.0	4.5743	2.2144	0.0448	0.9423	0.0711	0.0825	0.0085	2.1696	0.1638
MSA	2.5	3.8210	2.5921	0.0608	1.0345	0.0977	0.0936	0.0131	2.3821	0.2249
NOP	2.0	3.4608	1.9233	0.0678	0.9752	0.1037	0.0324	0.0051	2.2455	0.2389
RHA	2.0	3.4638	1.7973	0.0670	0.9104	0.0957	0.0408	0.0063	2.0962	0.2204
SEA	2.0	3.5277	2.3049	0.0450	0.9876	0.0757	0.0705	0.0073	2.2740	0.1744
WCB (Zone of GGF)	**3.5**	**3.5805**	**2.3567**	**0.1942**	**1.0336**	**0.1778**	**0.0548**	**0.0245**	**2.3799**	**0.4094**
ZFM	2.0	4.2720	2.0348	0.0547	0.9395	0.0840	0.0558	0.0070	2.1632	0.1935
ZML	2.0	3.8205	2.3235	0.0486	1.0279	0.0850	0.0532	0.0059	2.3668	0.1956

* values from Johnston et al. (1994)

Table 6.2: Gutenberg-Richter parameters for Model 2 (Verbeeck, 2009; modified Fugro, 2020)

Zone	Mmin (fit)	a (normalized to 106 km2)	a (scaled to area of zone)	σa	b	σb	λ (Mmin=3.5)	σ λ (Mmin=3.5)	β	σ β
Zone 1	2.0	3.6000	2.3209	0.0393	0.9390	0.0633	0.1082	0.0098	2.1622	0.1457
Zone 2	2.5	3.5447	1.9329	0.1121	0.9858	0.1398	0.0304	0.0078	2.2700	0.3220
Zone 3	3.5	5.2466	2.6100	0.1448	1.0331	0.1645	0.0987	0.0329	2.3787	0.3788
Zone 4	1.5	4.0573	2.2339	0.0325	1.0098	0.0596	0.0501	0.0037	2.3251	0.1372
Zone 5	3.0	4.4333	2.1579	0.1535	1.0179	0.1617	0.0394	0.0139	2.3438	0.3723
Zone 6	2.5	4.7589	1.8999	0.1121	0.9734	0.1375	0.0311	0.0080	2.2412	0.3167
Zone 7	2.0	4.4081	2.2301	0.0396	0.8995	0.0605	0.1207	0.0110	2.0712	0.1394
Zone 8	2.5	3.9399	1.2908	0.2171	0.9601	0.1749	0.0085	0.0043	2.2106	0.4027
Zone 9	2.0	3.7263	1.3160	0.1254	0.9401	0.1454	0.0106	0.0031	2.1647	0.3348
Zone 10	2.0	3.2631	1.6333	0.0906	0.9567	0.1236	0.0193	0.0040	2.2028	0.2846
Zone 11	1.5	4.6191	1.8102	0.0279	0.9535	0.0479	0.0297	0.0033	2.1954	0.1102
Zone 12	1.5	4.6191	2.0958	0.0279	0.9535	0.0479	0.0574	0.0045	2.1954	0.1102
Zone 13	1.5	3.5499	1.2510	0.0887	0.9410	0.1221	0.0091	0.0019	2.1668	0.2812
Zone 14	2.5	4.3578	2.2338	0.0806	0.9914	0.1152	0.0581	0.0108	2.2827	0.2652
Zone 15	3.5	3.6900	2.4904	0.1942	1.0702	0.1790	0.0555	0.0248	2.4642	0.4121
Zone 16	2.5	3.7817	2.5356	0.0620	1.0196	0.0978	0.0927	0.0132	2.3477	0.2251
Zone 17	2.5	3.7312	2.6013	0.0486	0.9636	0.0756	0.1693	0.0189	2.2188	0.1741
Zone 18	2.0	4.8563	3.1952	0.0253	1.1764	0.0571	0.1196	0.0070	2.7087	0.1314
Zone 19	2.5	3.7842	1.7088	0.1448	0.9850	0.1560	0.0183	0.0061	2.2680	0.3592
Zone 20 (Zone of GGF)	**1.8**	**3.6224**	**2.5094**	**0.0287**	**0.9861**	**0.0509**	**0.1143**	**0.0076**	**2.2706**	**0.1172**
Zone 21	2.5	2.4941	1.1417	0.3071	1.0178	0.1880	0.0038	0.0027	2.3435	0.4329
Zone 22	2.5	3.2211	1.6385	0.1942	1.0556	0.1755	0.0088	0.0039	2.4305	0.4040
Zone 23	2.5	3.3843	2.2117	0.0806	0.9830	0.1136	0.0590	0.0110	2.2634	0.2616

6.2.3 Induced Model

Dynafrax modelled the possible earthquakes that might happen depending on four different injection scenarios (Figure 6.1).

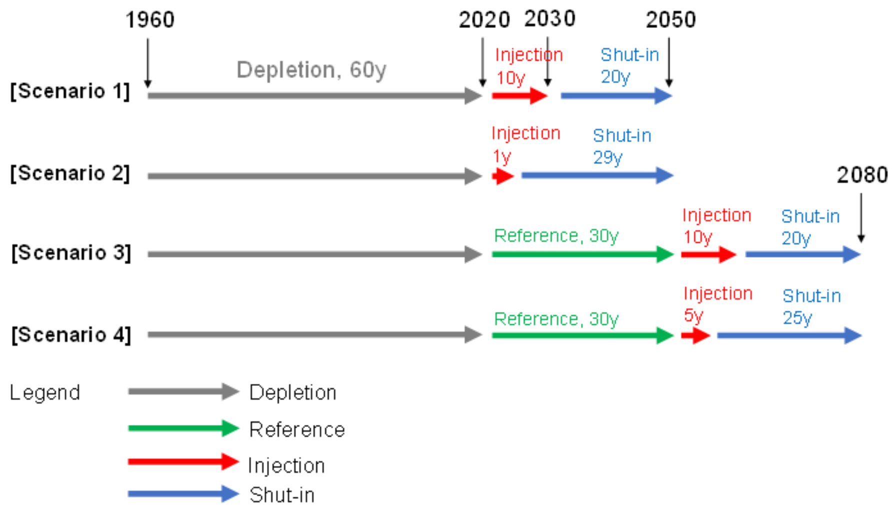

Figure 6.1: Timeline showing the depletion, reference (when applicable indicate that no injection was performed), injection and shut-in periods for injection scenarios 1-4 (*from Figure 7-4 of the Dynafrax report (October 2021)*).

Figure 6.1 shows the different scenarios modelled in this study. This figure is coming from the report of Dynafrax UG. They explain that the four injection scenarios, denoted cases 1-4, were simulated, each beginning after the depletion period had run for its entire 60 year duration. Injection was simulated from nine wells. For cases 3 and 4, injection was preceded by a 30-year reference period, where pressure was allowed to naturally recover. Depending on the case, the rates of injection will be faster (scenario 2 or 4) or slower (scenario 1 or 3).

As explained previously, we will calculate from the simulated earthquakes a Gutenberg-Richter model which will be valid only for a considered period of time.

Due to the scarcity of data, a classical fit of the GR law is not possible therefore we used an alternative approach:

- For the *b-value*, we assume a *b-value* equal to 1 (global average value observed in seismotectonic and induced sources around the world).
- For the *a-value* calculation, we initiate our model at a M_{fit} of 1.0, 1.5 and/or 2.0. And we use the mean a-value of the three Mfit.

We obtain 8 possible recurrence models as shown on Figure 6.2 depending if we choose a period representing the injection time only (1, 5 or 10 years depending on the scenarios) or a period representing the injection time plus the shut-in period (30 years for all scenarios).

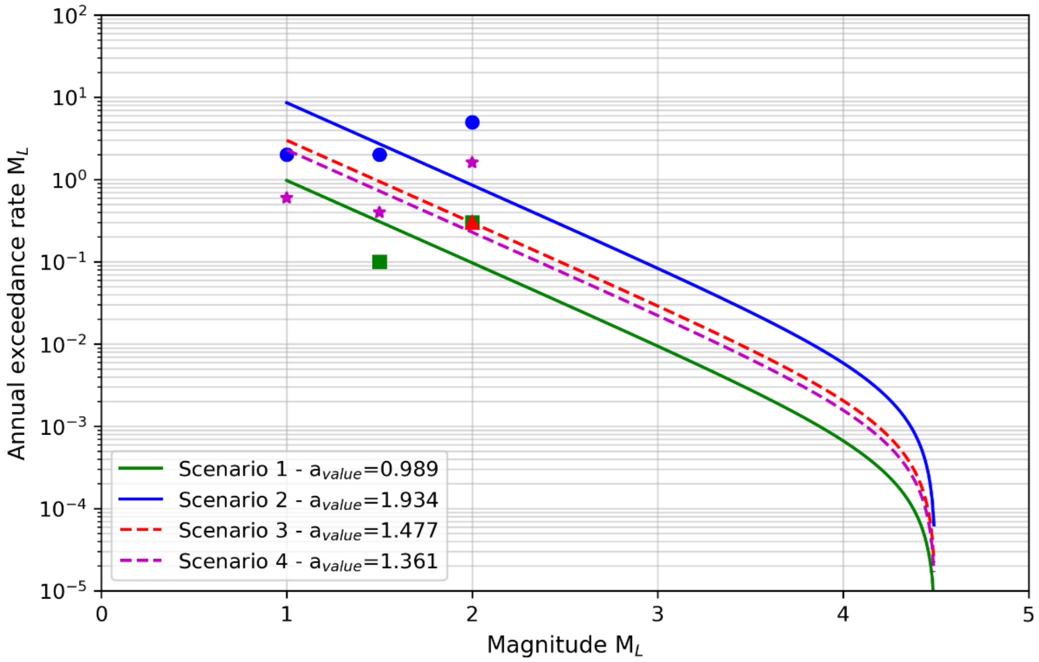

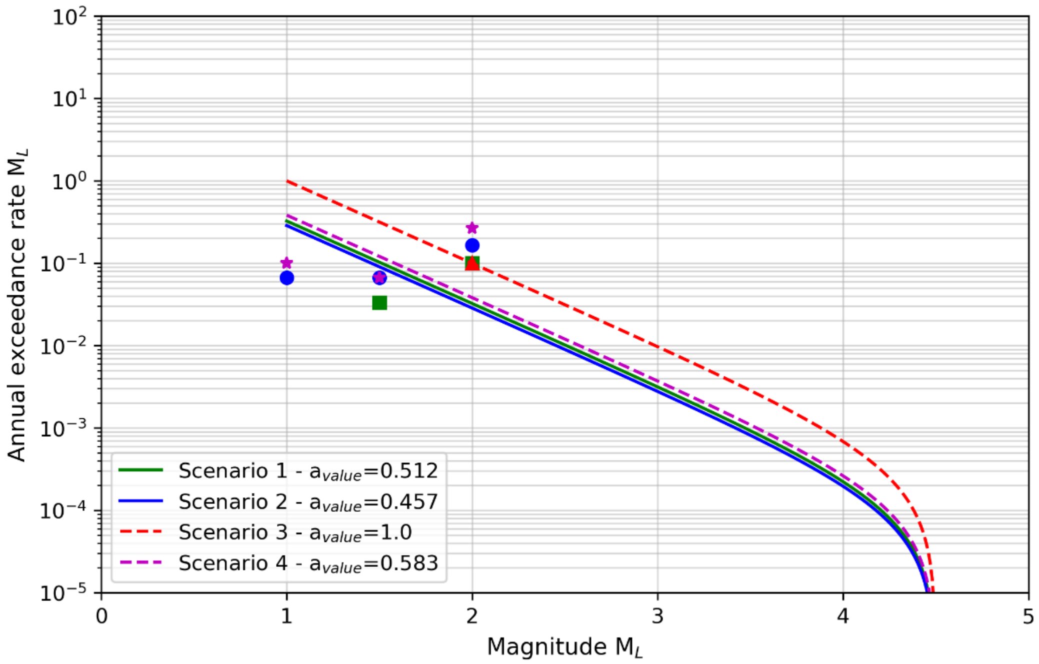

Figure 6.2: Gutenberg-Richter models for the four scenarios (1-2-3-4) with a mean a-value of all the different Mfit (1.0, 1.5 or 2.0 depending on the scenarios). Top: rates calculated over the injection time only (1, 5 or 10 years depending on the scenarios). Bottom: rates calculated over the injection time + shut-in period (30 years for all scenarios).

The mean a-value for each scenario and for each period of injection is:

- Scenario 1: a_{value}=0.989 (T=10 years) and a_{value}=0.512 (T=30 years)
- Scenario 2: a_{value}=1.934 (T=1 year) and a_{value}=0.457 (T=30 years)
- Scenario 3: a_{value}=1.477 (T=10 years) and a_{value}=1.0 (T=30 years)
- Scenario 4: a_{value}=1.361 (T=5 years) and a_{value}=0.583 (T=30 years)

We compare our scenarios with the recurrence models from each host zone (WCB and Zone 20) for the seismotectonic models SSC1 and SSC2, respectively. We normalize our *a-value* to $1x10^6$ km^2 for comparison.

We observe that we have higher normalized rates for the recurrence models based on induced seismicity **using the injection period of time only** (Figure 6.3). This means, the number of earthquakes of M=2.0 per km^2 is higher (between 2 and 20 times) in the induced source than in the seismotectonic zone where Groningen is situated (Figure 6.3).

The annual activity rate of earthquakes with magnitude equal or greater than 2.0 per km^2, $\lambda_{2.0}$, is:

- SSC1 (WCB): 3.26069×10^{-5}
- SSC2 (Zone 20): 4.46874×10^{-5}
- Scenario 1: 8.01801×10^{-5}
- Scenario 2: 7.06426×10^{-4}
- Scenario 3: 2.46642×10^{-4}
- Scenario 4: 1.88828×10^{-4}

On Figure 6.4, where the period is increased (injection time + shut-in period), we notice that scenarios 1, 2 and 4 have similar normalized rates for the recurrence models based on induced seismicity than those based on the seismotectonic models SSC1 and SSC2. Indeed, we increase the period from 1, 5 or 10 years up to 30 years, significantly reducing the rates.

The value of $\lambda_{2.0}$ per km^2 is:

- SSC1 (WCB): 3.26069×10^{-5}
- SSC2 (Zone 20): 4.46874×10^{-5}
- Scenario 1: 2.67342×10^{-5}
- Scenario 2: 2.35541×10^{-5}
- Scenario 3: 8.22368×10^{-5}
- Scenario 4: 3.14823×10^{-5}

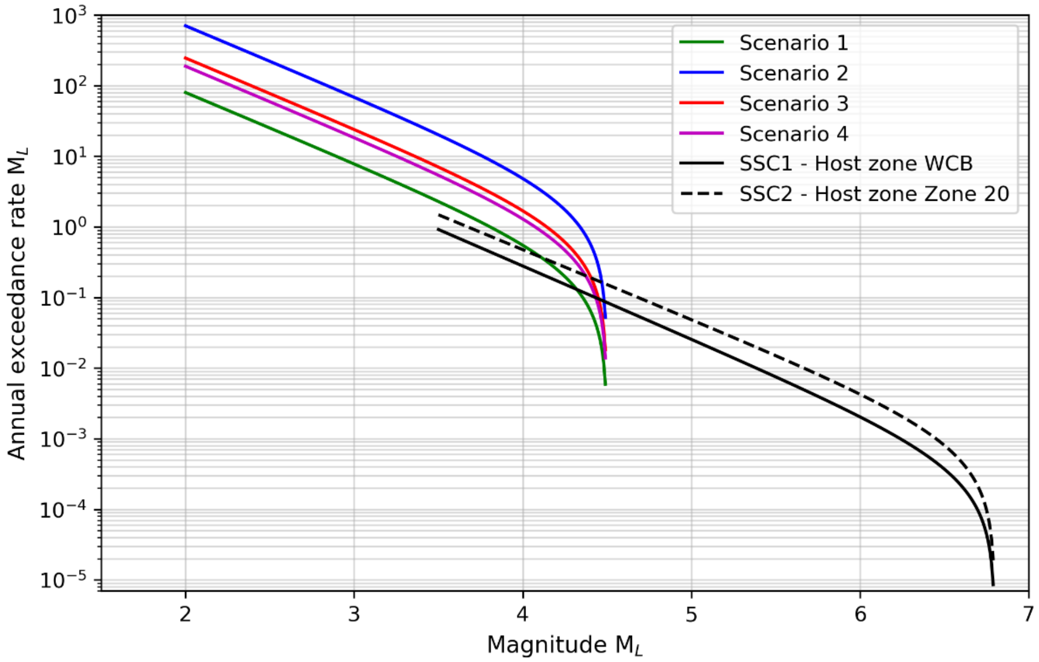

Figure 6.3: Comparison between the mean Gutenberg-Richter models of the four scenarios (1-2-3-4) with the GR models of the seismotectonic models SSC1 and SSC2 for a period of 1, 5 or 10 years (injection time only) depending on the scenarios.

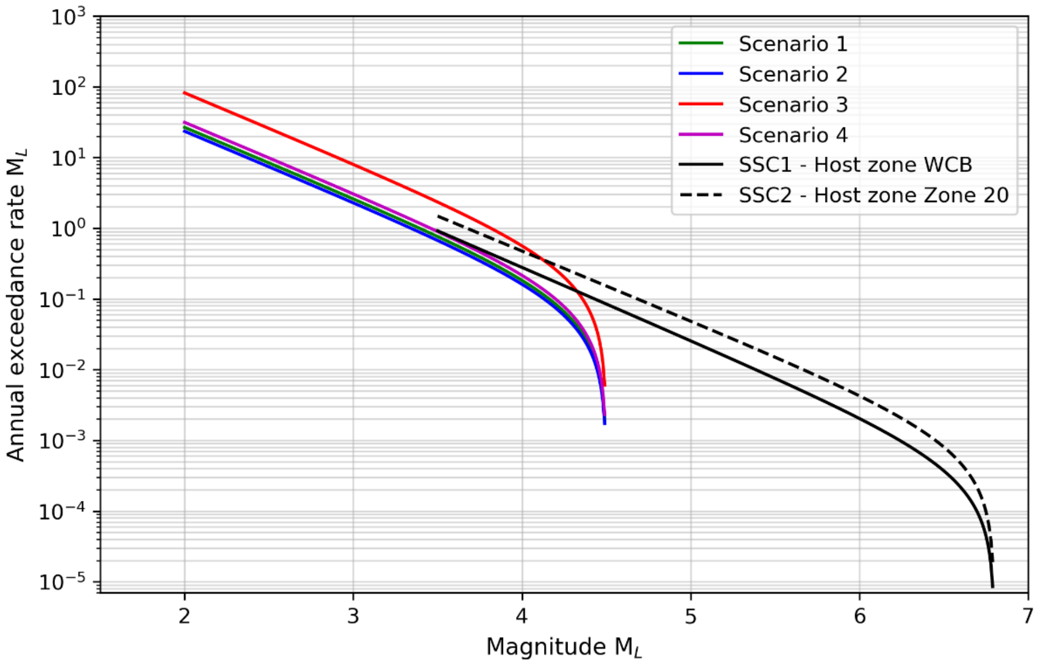

Figure 6.4: Comparison between the mean Gutenberg-Richter models of the four scenarios (1-2-3-4) with the GR models of the seismotectonic models SSC1 and SSC2 for a period of 30 years (injection time + shut-in).

7. Ground Motion Prediction Equations

7.1 Selection of GMPEs for seismotectonic sources

Ground Motion Prediction Equations (GMPEs or attenuation relationships) appropriate for the seismotectonic context are selected with the objective to capture the epistemic uncertainties and to fulfill the criteria of inclusiveness and exhaustiveness of the alternatives.

The area of interest being located in a region of low seismic activity seen in the SHARE project as a transition zone between active crustal regions of southern Europe and stable continental regions of northern Europe, GMPEs from these two seismotectonic contexts have been used. The set of selected GMPEs is given below with a description of the models:

- **Akkar *et al.* (2014).** This model corresponds to one of the most recent GMPEs developed for the Euro-Mediterranean regions and it represents the evolution of the Akkar & Bommer (2010) GMPE selected in both SHARE and GEM projects.;
- **Bindi *et al.* (2017):** This model was specifically developed for an application of PSHA in low to moderate seismicity areas, such as northwestern Europe.;
- **Campbell & Bozorgnia (2014):** This model is also one of the five NGA models (New Generation of Attenuation relationship) of second generation. It can be considered as the natural evolution of Campbell and Bozorgnia (2008).;
- **Cauzzi *et al.* (2015)**: This is an update of Cauzzi & Faccioli (2008) model resulting from the exploitation of a worldwide database recorded in crustal active regions and mainly composed of Japanese data;
- **Yenier and Atkinson (2015):** This model is one of the most recent GMPE adapted to stable continental seismic zones. It has been developed in two distinct steps: first a generic model has been developed based on stochastic data, with parameters calibrated on records of Californian events.

The use of the 5 selected GMPEs allows a full propagation of the epistemic uncertainties associated with the GMPEs.

Table 7.1 summarizes the main characteristics of the selected GMPEs and their validity domains.

7.2 Selection of GMPEs for induced seismicity sources

The attenuation of the ground motion originated by induced sources is typically different from the attenuation observed in seismotectonic sources. Moreover, in Groningen, site-specific GMPEs were fitted using local seismic data recorded.

Then, we tested 4 GMPEs developed in the context of induced seismicity:

- **Atkinson (2015)**: induced GMPE from the NGA-West2 database for earthquakes between $3.0<M_W<6.0$ and at distances below 40 km
- **Bindi *et al.* (2017)**: developed for stable areas and low to moderate seismicity areas
- **Bommer *et al.* (2016)**: updated from Dost *et al.* 2004 and developed specifically for the Groningen Gas Field.
- **Dost *et al.* (2004)**: induced GMPE developed in Netherlands (Groningen area) for earthquakes between $1.0<M_L<5.0$ with the Bommer *et al.* 2013 adaptation

Their comparison, through a Trellis Plot is represented on Figure 7.1.

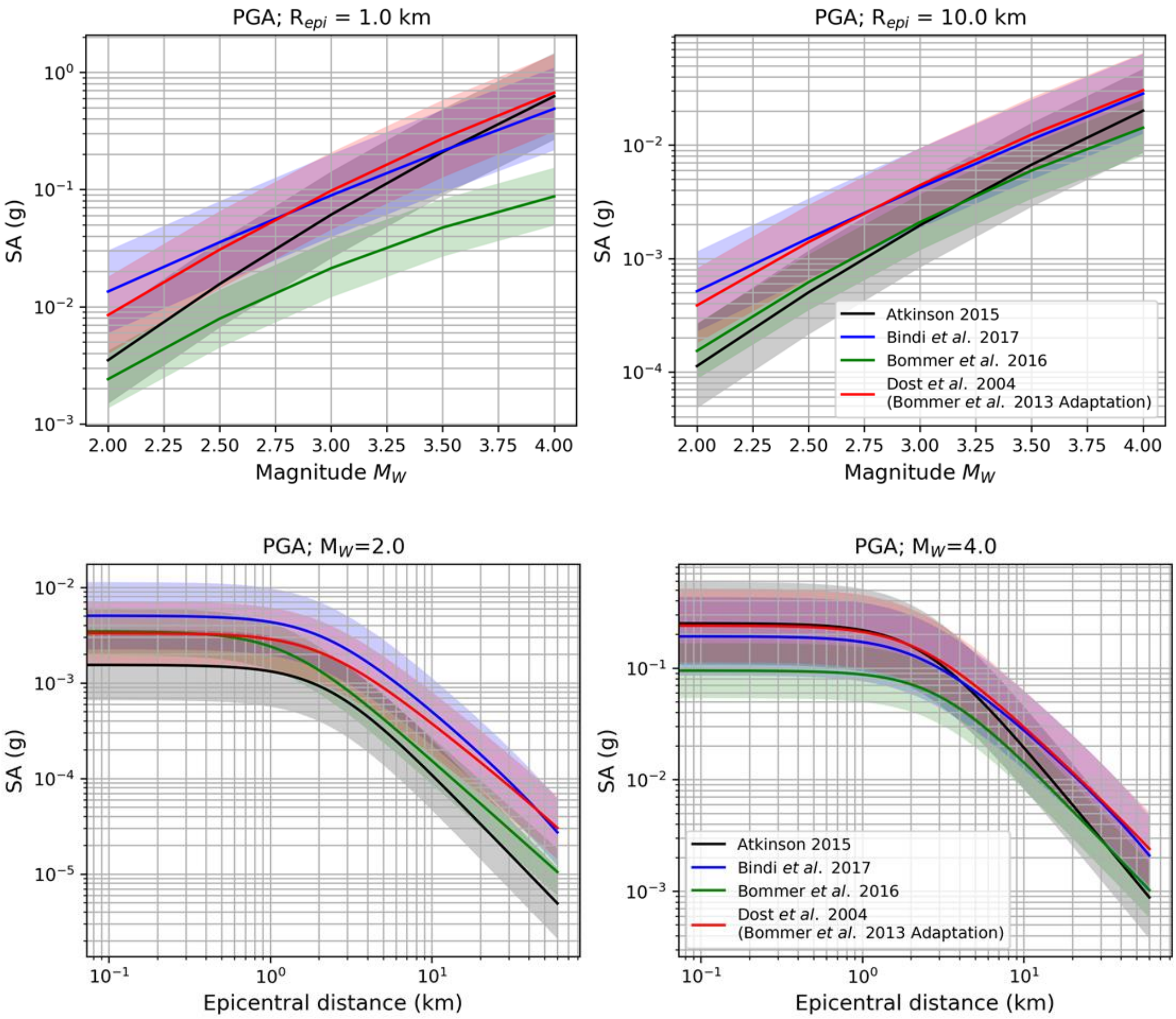

Figure 7.1: Trellis Plots at PGA for the induced GMPEs. Top: Acceleration versus epicentral distance for M_W=2.0 (left) and M_W=4.0 (right). Bottom: Acceleration versus magnitude for R_{epi}=1 km (left) and R_{epi}=10 km (right). Black line: Atkinson 2015, blue line: Bindi et al. 2017, green line: Bommer et al. 2016 and red line: Dost *et al.* 2004 (Bommer *et al.* 2013 adaptation)

Finally, we performed the seismic hazard calculations using the Bommer *et al.* 2016 GMPE, which corresponds to the most recent and detailed GMPE specifically developed for induced seismicity in Groningen.

Table 7.1: Characteristics of the selected GMPEs for the site-specific PSHA to the GGF.

GMPE	Region database	Type	Magnitude range	Distance range	Period range	Site classification	Region of application
Akkar et al. (2014)	Euromediterranean area, Middle East	Empirical	Mw=4.0-7.6	Rhypo, Rrup, Repi* = 1-200 km.	PGA; 0.01-4 s	Function of V_{S30}	Active shallow crustal region
Bindi et al. (2017)	Worldwide	Empirical	Mw=3.0-8.0	Rhypo, Rjb = 0-300 km.	PGA; 0.01-4 s	Function of V_{S30}	Stable region
Campbell & Bozorgnia (2014)	Worldwide	Empirical	Mw=3.3-8.5	Rrup = 0-300 km.	PGV, PGA; 0.01-10 s	Function of V_{S30}	Active shallow crustal region
Cauzzi et al. (2015)	Worldwide – mostly Japan	Empirical	Mw=4.5-7.9	Rrup =0-150 km	PGA; 0.01-10 s	EC8 site class or Function of V_{S30}	Active shallow crustal region
Yenier & Atkinson (2015)	US (stochastic data) (CEUS)	Stochastic	Mw=3.0-8.0	Rrup =1-600 km	PGA; 0.01-10 s	Function of V_{S30}	Stable region

*Rhypo = Hypocentral distance, Rrup = closest distance to the rupture, Repi = Epicentral distance

8. Modelling Induced Seismicity

8.1 Global Probabilistic Logic Tree

The approach using logic trees allows using alternative models. A weighting factor is assigned for each alternative model. It is interpreted as the relative confidence of that specific model being the correct one. The logic tree consists of a series of nodes, representing points at which models are specified, and branches that represent the different models specified at each node. The sum of the probabilities of all branches connected to a given node is 1.

The weights assigned to the main branches of the logic tree associated with seismotectonic models and GMPEs are as follows (Figure 8.1):

- For the seismotectonic models: an equal weight of 1/2 is assigned to each seismotectonic model;
- For the GMPEs:
  - those that can be applied more specifically for the European context are weighted to represent 50% of the logic tree. An equal weight of 25 % is assigned to each of these GMPEs (Akkar *et al.* 2014, Bindi *et al.* 2017);
  - a 40% weight is associated for the two models (Campbell and Bozorgnia 2014, Cauzzi *et al.* 2015) developed in Active Crustal Shallow regions (ASCRs) which are calibrated on a large database of worldwide records. An equal weight of 20% is assigned to each one.
  - a 10% weight is associated to the remaining model developed for Central Eastern North America (Yenier and Atkinson, 2015) expressing less confidence in its applicability in the region of interest.

This weighting scheme was adopted from an Offshore Windfarm PSHA, performed by Fugro in 2020.

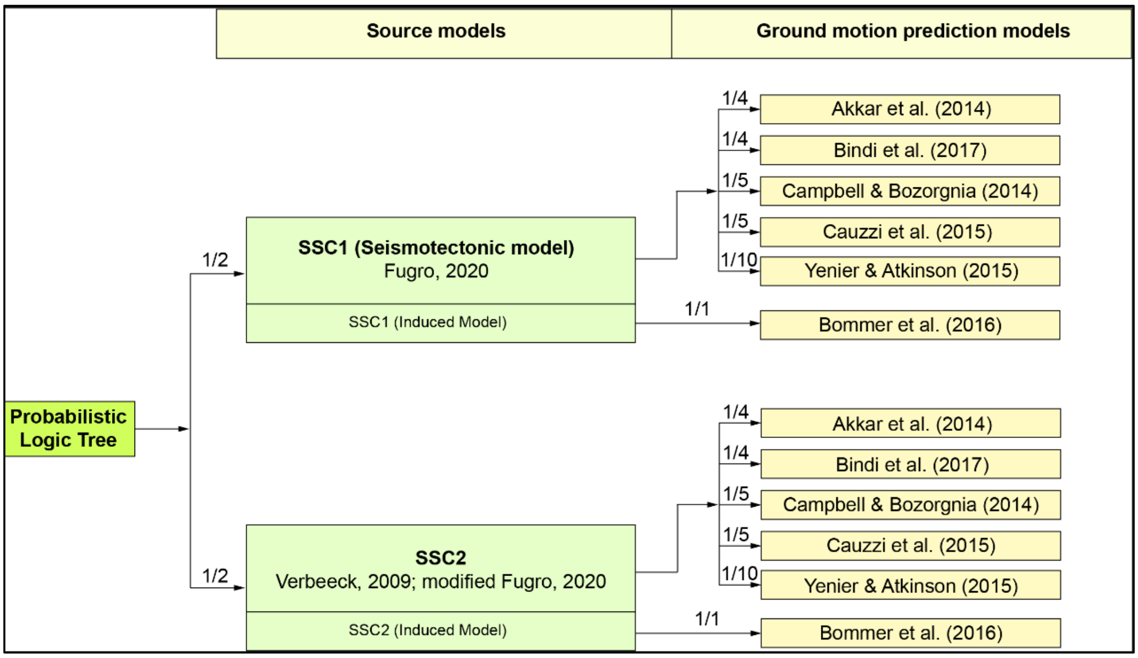

Figure 8.1: Logic tree developed for the probabilistic seismic hazard assessment of seismotectonic model at the Groningen site.

8.2 Common hypotheses

The common hypothesis taken into account, for all branches of the logic tree are:

- A minimum magnitude M_{min} = 3.5 (M_W) for the calculation of the seismic hazard for the seismotectonic models. For regions with low seismic activity (or when low return periods are analyzed), this is a usual value and it is retained here in order to take into account all magnitude contributions.
- A minimum magnitude of M_{min} = 2.0 (M_W) for the calculation of the seismic hazard for the induced model. This value was selected to take into account the induced earthquakes considered able to produce damages. The lower magnitudes are not considered able to produce damages in the structures and were not considered in the PSHA calculations. Moreover, magnitudes higher than 2.0 are in the domain of validity of GMPEs used for induced sources. Finally, we have to note that this value (2.0) is significantly lower than the 3.5 considered in seismotectonic sources because the induced earthquakes typically occur close to the surface (hypocenters with small depth) and, therefore, lower magnitudes of induced earthquakes can produce more seismic ground motion at surface than same magnitudes of natural earthquakes. In any case, the choice of M_{min} = 2.0 (M_W) is always subjective and based in the previously cited considerations.
- Integration up to 3 standard deviations of the GMPEs (-3σ to 3σ). This is a commonly accepted truncation value in PSHA practice for industrial projects.
- The integration distance used is 300 km.
- A shear wave velocity over the top 30 meters V_{S30} equal to 200 m/s.
- For the induced model, we specify the M_{max}=4.5. The uncertainty in this value is large. The maximum observed magnitude in Groningen is 3.6 and the maximum magnitude coming from the different scenarios never exceeds 3.0. Therefore, the adoption of M_{max}=4.5 can be considered as a conservative approach and it correspond to other M_{max} considered in similar projects producing induced seismicity (i.e geothermal projects).

We compute the hazard at PGA only.

The hazard is computed using the software R-CRISIS (Ordaz et al., 2018). R-CRISIS has been tested and validated in the PEER project Hale et al. (2018), where different seismic hazard codes were analysed.

8.3 Probabilistic Seismic Hazard Results

The results of the probabilistic seismic hazard analysis consist of seismic hazard curves for the PGA, at the center of the Groningen Gas Field. The statistical analysis of the hazard curves from all the logic tree branches leads to the definition of the mean hazard curves.

8.3.1 Seismic Hazard Curve at PGA for Groningen Gas Field

Figure 8.2 (top and bottom) shows the mean seismic hazard curves of the seismotectonic model at PGA for the Groningen Reservoir (black line). We compare this result with the impact of adding the induced scenarios with a period of injection time only (top of Figure 8.2) or with a period of injection time + shut-in (bottom of Figure 8.2) for the gas field (green, blue, red and magenta lines).

We observe significant differences between the seismotectonic models and the induced models for the reduced period of injection (T=1, 5 or 10 years). For example, at 475-year, for the smallest scenario (# 1), the acceleration is increased 1.3 times and for the strongest scenario (# 2), the acceleration is increased 2.6 times, while remaining at a very low value of 0.04 g at PGA if we assume a return period of 475 years for the worst case scenario (then, assuming stationarity of the seismicity).

However, for the case of a longer period of injection (T=30 years, Figure 8.2 – bottom), at 475 years return period, for the smallest scenario (# 2), the acceleration is increased 1.1 times and for the strongest scenario (# 3), the acceleration is increased 1.3 times only.

Therefore, the introduction of an induced zone source (even with very few and weak earthquakes) will increase the seismic hazard.

However, we emphasis 3 important considerations:

1. The comparison between the seismotectonic model and scenarios of induced seismicity is valid only for the next 1, 5 or 10 years (depending on the period of injection of each scenario) or for the second case, 30 years (period of injection + shut-in for all scenarios). After those periods, the seismicity is supposed to return to its natural period. The induced seismicity is time dependent, without injection, there is no seismicity.
2. Even considering the induced seismicity, the acceleration levels higher than 0.1 g have annual probabilities of exceedance lower than 0.0002. This means that the seismic hazard is significantly increased but the probability to have higher accelerations remains low. The increase in seismic hazard is basically associated with the very low natural seismicity of Groningen. Then, even a little induced seismicity produces a non-negligible increase of seismic hazard.
3. The hazard curves from the different scenarios in Figure 8.2 are only valid for the next 1, 5, 10 or 30 years. In the context of induced seismicity, those hazard curves are not stationary. The accelerations at 475 years return period (and others) are only informative and valid only for the seismotectonic seismic hazard.

We should also note that compared to the previous offshore windfarm project performed by Fugro, we obtain a higher value of acceleration at PGA at 475 years for the mean model because we reduced the minimal magnitude considered in the PSHA, M_{min}, at 3.5 instead of 4.5 in order to take into account the induced seismicity. It means that in our calculations, we are taking into account that magnitudes from 3.5 to 4.5 can produce accelerations. In the offshore wind farm project, we considered a M_{min}=4.5, the most typical value used in industrial projects, because we consider than magnitudes lower than 4.5 cannot produce damages in new structures.

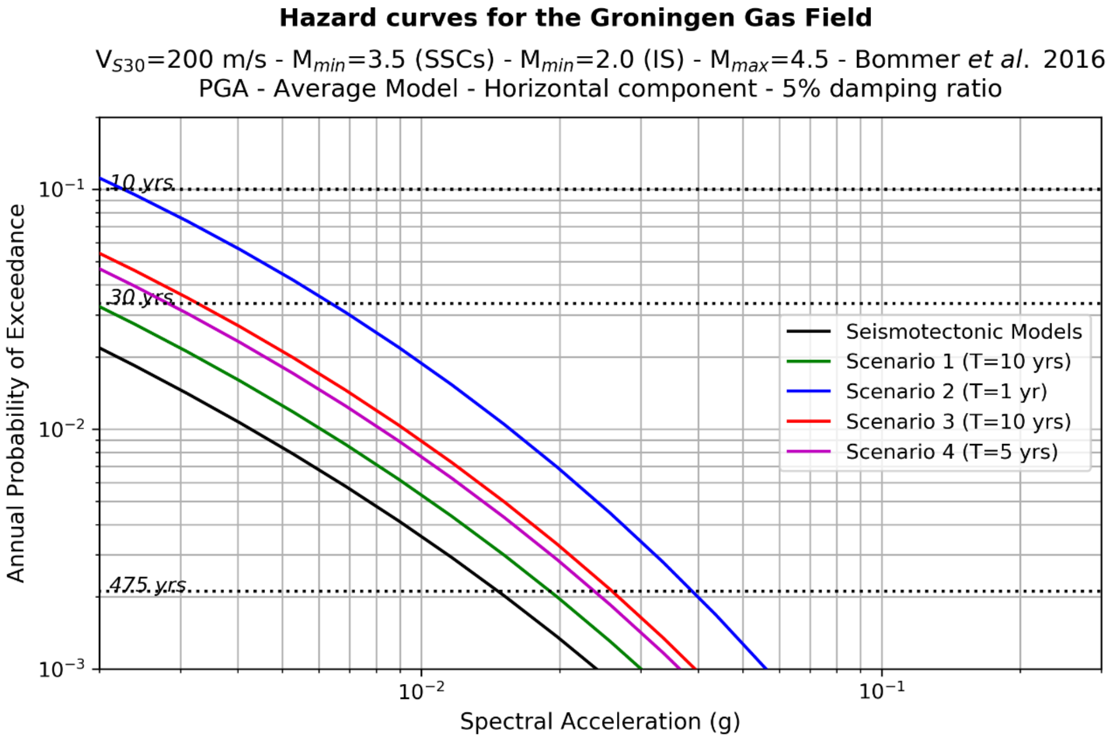

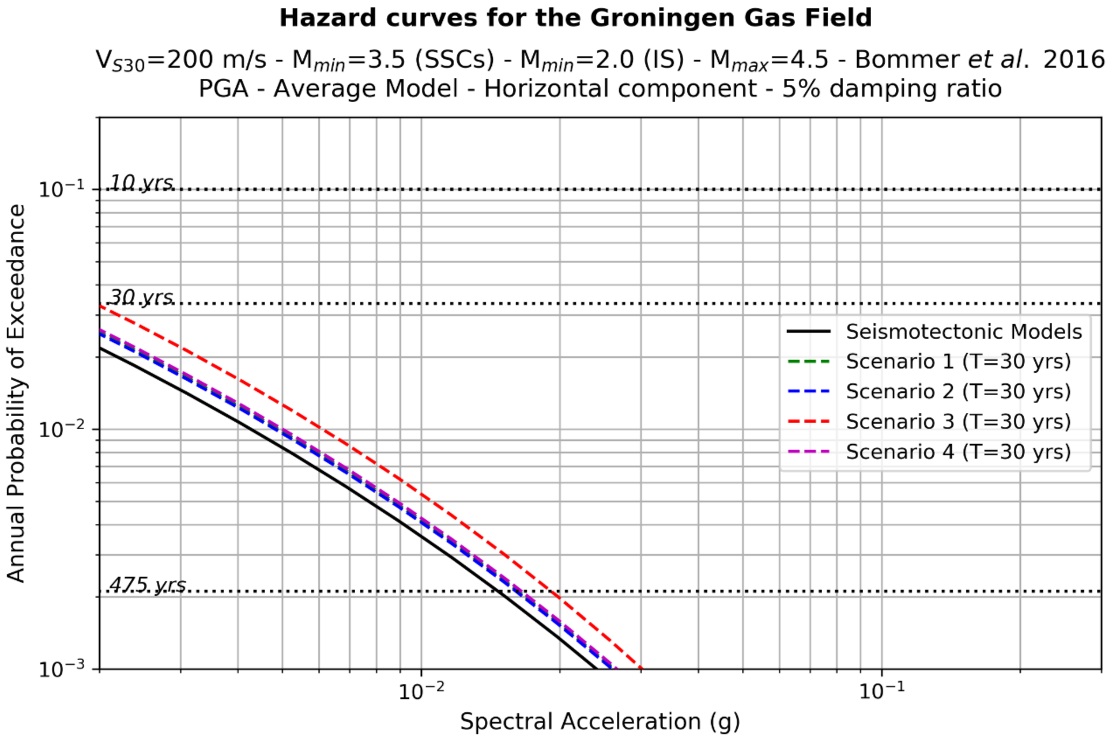

Figure 8.2: Groningen Reservoir site – Top: Mean seismic hazard curves calculated with a period related to the injection time only (T=1, 5, 10 years). Bottom: Mean seismic hazard curves calculated with a period related to the injection time + shut-in period (T=30 years) – Horizontal component, V_{S30} = 200 m/s, 5 % damping. Induced GMPE: Bommer *et al.* 2016. Note: the return periods are shown only for information and they can only be considered for the seismotectonic model.

Other representation of the results by scenarios directly comparing the difference in period of injection (10 vs 30 years for scenario 1, for example).

The previous Figure 8.2 can also be represented through Figure 8.3, comparing the periods of injection scenario by scenario.

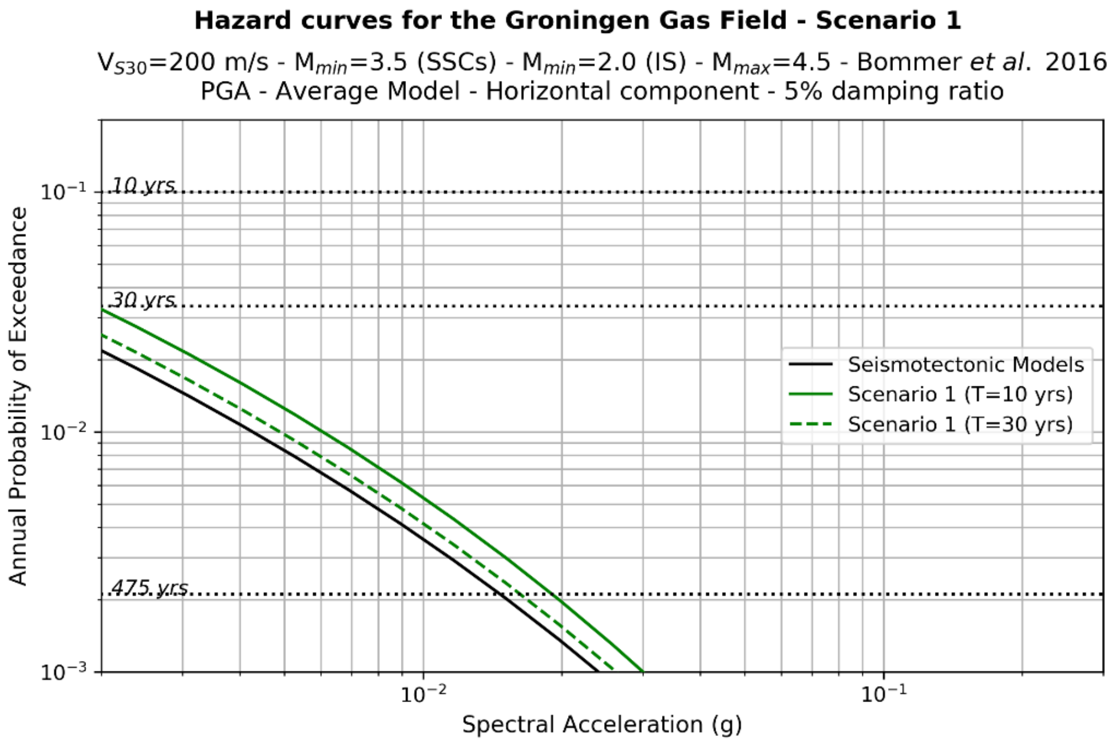

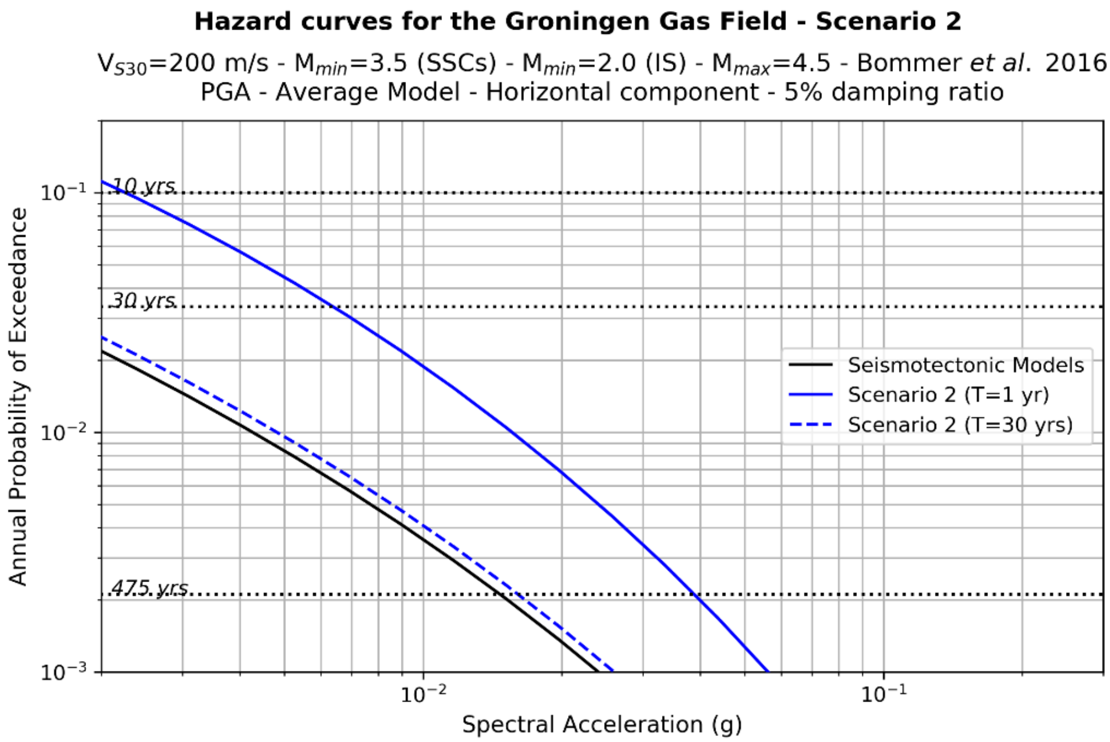

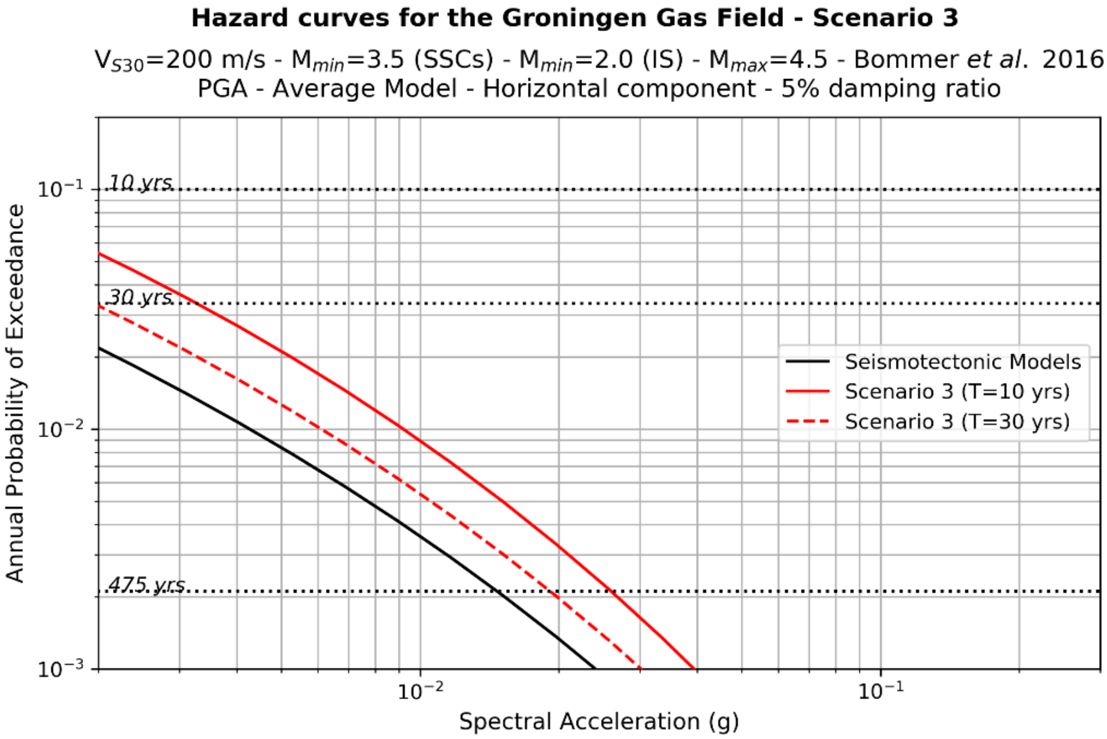

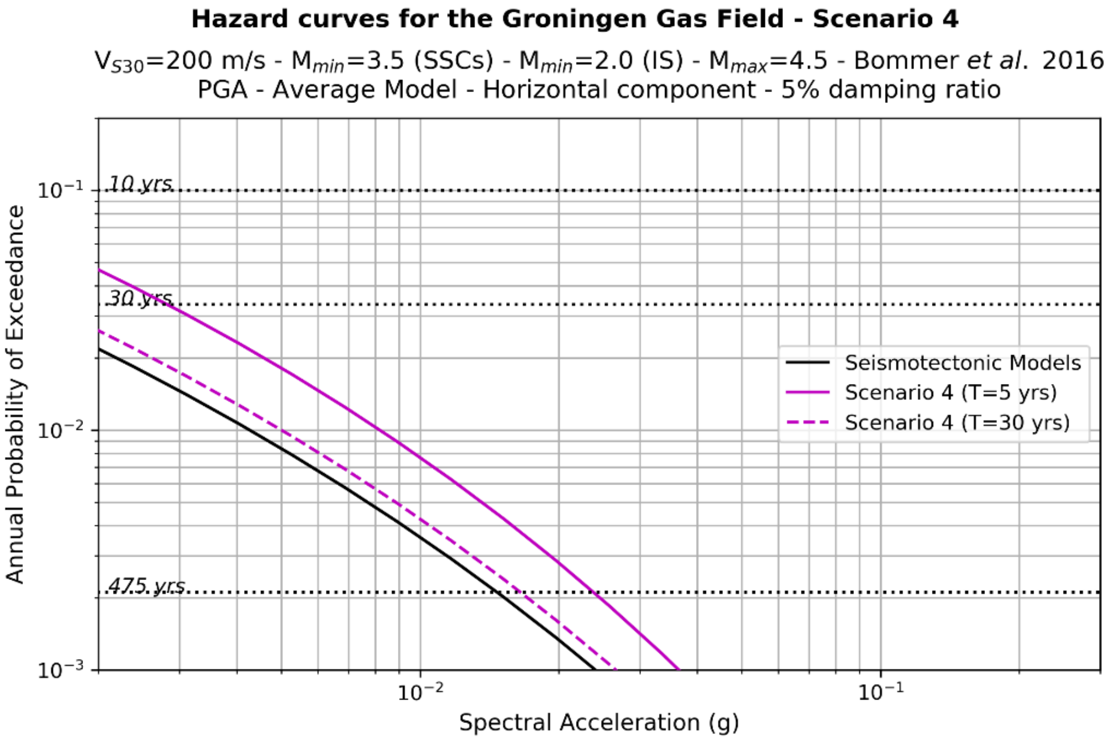

Figure 8.3: Mean seismic hazard curves for the Groningen Reservoir site. From Top to Bottom: Scenario 1, Scenario 2, Scenario 3, Scenario 4. Comparison with the period of injection only (10, 1, 10 and 5 years respectively) and the period of injection + shut-in (30 years) – Horizontal component, V_{S30} = 200 m/s, 5 % damping. Induced GMPE: Bommer *et al.* 2016. Note: the return periods are shown only for information and they can only be considered for the seismotectonic model.

8.3.2 Sensitivity analysis for M_{max}

In Figure 8.4 we compare for the scenario 1, the hazard curves using different M_{max} from 4.5 to 5.0. We don't not a major difference between the two different M_{max}. Small differences will be visible for lower annual probability of exceedance.

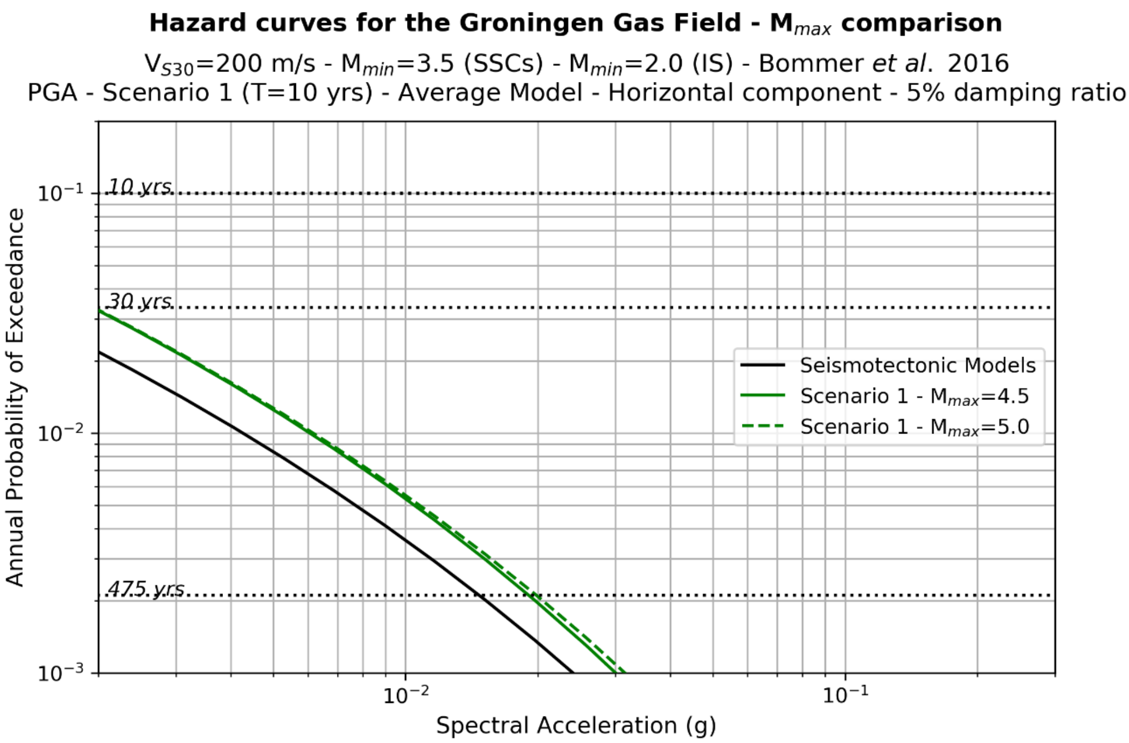

Figure 8.4: Hazard curves for the Groningen Reservoir at PGA for V_{S30}=200 m/s. Comparison of different M_{max} used for the induced scenario 1. In green solid line: M_{max}=4.5, dashed line: M_{max}=5.0.

8.3.3 Sensitivity analysis for GMPEs

In Figure 8.5 we compare for the scenario 1, the hazard curves using different induced GMPEs.

We note for induced GMPEs that Dost *et al.* 2004 gives, with Bindi *et al.* 2017, the strongest results whereas Bommer *et al.* 2016 predict smaller accelerations. This is coherent with the Trellis Plot in Figure 7.1.

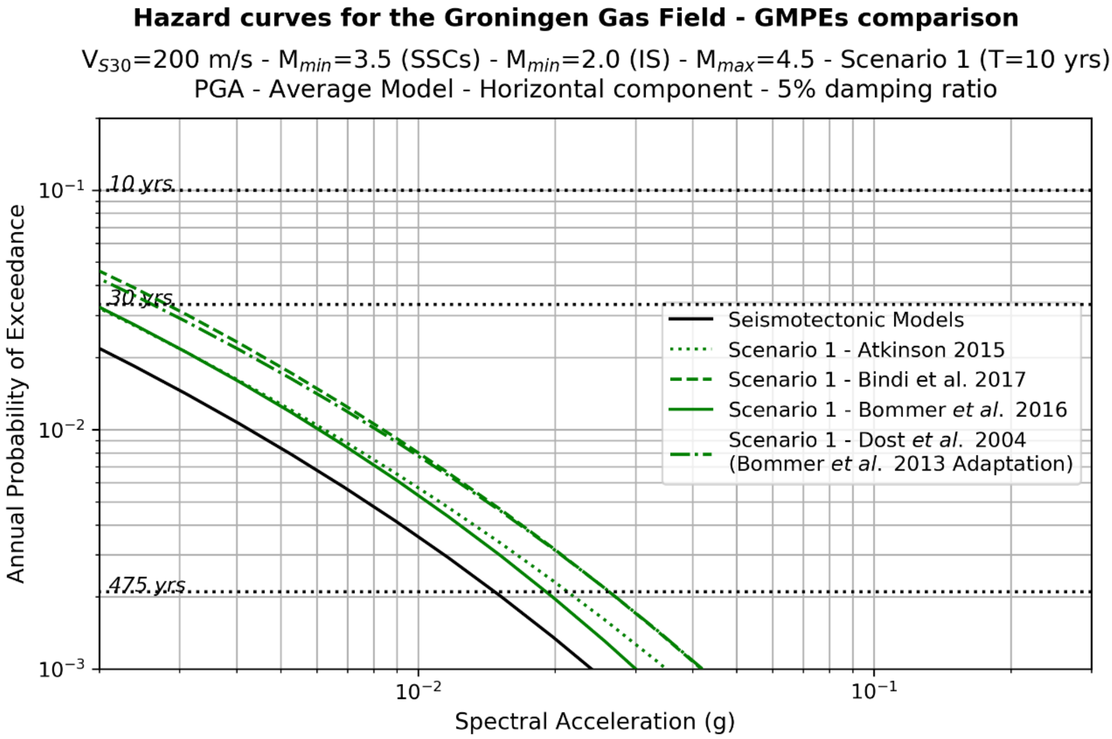

Figure 8.5: Hazard curves for the Groningen Reservoir at PGA for V_{S30}=200 m/s. Comparison of different induced GMPEs with the seismotectonic model. Dotted line: Atkinson 2015, dashed line: Bindi et al. 2017, solid line: Bommer *et al.* 2016, dashdot line: Dost *et al.* 2004 (Bommer *et al.* 2013 adaptation).

8.3.4 Sensitivity analysis for M_{min}

The Figure 8.6 presents the comparison between the use of M_{min}=2.0 and M_{min}=3.5 for both the seismotectonic models and the induced seismicity models.

The black arrow represents the difference in M_{min} between the seismotectonic models only. We observe that including earthquakes between 2.0 and 3.5 has an impact on the acceleration only for small probability of exceedance.

The blue arrow also represents the difference in M_{min} between the seismotectonic models but with the induced model. As the induced model doesn't dominate the hazard, we can find almost the same differences between the seismotectonic models with a M_{min}=2.0 or 3.5.

The green arrow represents the difference in M_{min} for the induced model between 2.0 and 3.5, while the seismotectonic models have a M_{min}=3.5. We see that adding earthquakes of magnitude 2.0<M_W<3.5 has an impact until a return period of 475 years. After 475 years, we don't see any differences.

To sum up this figure shows that the use of a weak M_{min} increases the annual probability of exceedance only for the weak accelerations (PGA< 0.06g). For PGA>0.06, the seismic hazard curves defined using both M_{min} are almost equivalent (the small differences observed are produced mainly for numerical differences occurring during the integration process of the hazard integral).

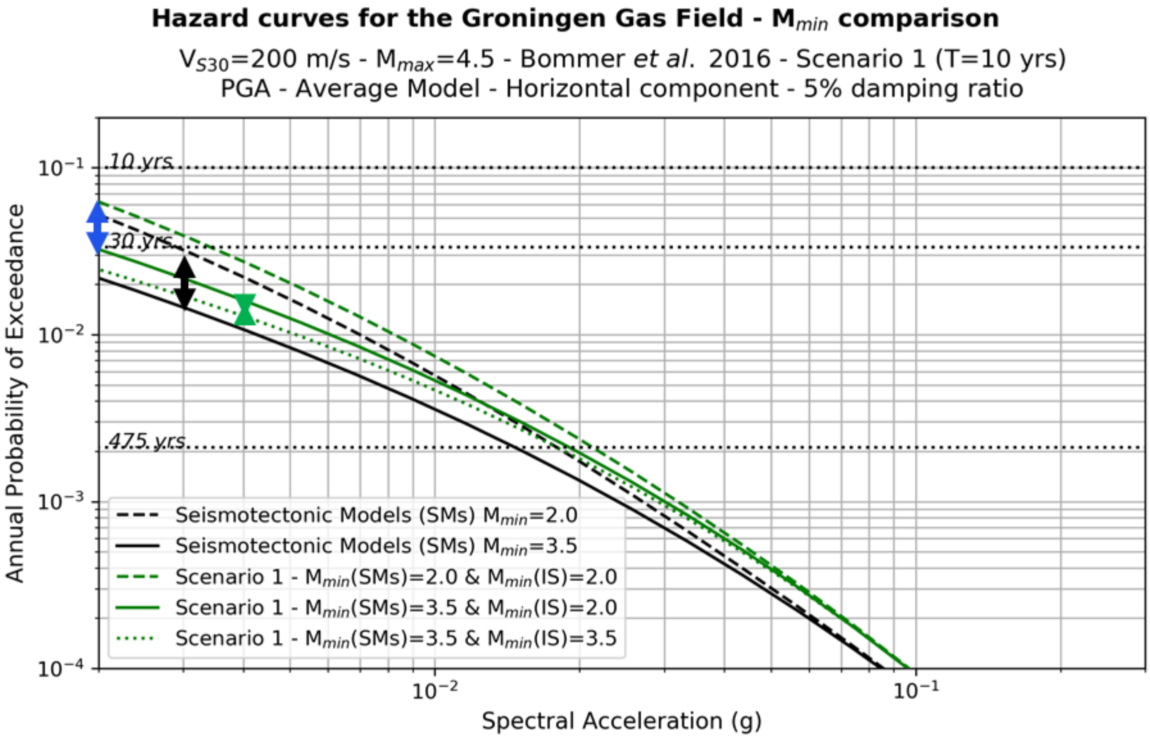

Figure 8.6: Comparison of different M_{min} used for the scenario 1 using 10 years of injection time. Groningen Reservoir site - Mean seismic hazard curves at PGA - Horizontal component, V_{S30} = 200 m/s, 5 % damping. Induced GMPE: Bommer *et al.* 2016.

9. Conclusion

To explore the effect of the induced seismicity produced by the induced seismicity predicted by the injection modelling used (using 4 scenarios), 2 site-specific probabilistic seismic hazard analysis (PSHA) with and without consideration of induced seismicity were performed for the Groningen Gas Field in Netherlands

The seismotectonic hazard model includes:

- 2 seismotectonic models:
  - A model specifically developed for this project (FUGRO, 2020);
  - A model adapted from the Verbeeck *et al.* (2009) model developed for Belgium;
- 5 Ground-Motion Prediction Equations (GMPEs):
  - Akkar et al. (2014);
  - Bindi et al. (2017);
  - Campbell & Bozorgnia (2014);
  - Cauzzi et al. (2015);
  - Yenier & Atkinson (2015).

The induced model considered includes:

- A zone source covering the Groningen Gas field (1216 km^2), where we consider that the induced seismicity is homogeneous
- The GMPE developed by Bommer *et al.* 2016 specifically developed for Groningen site.

The comparison of seismic hazard assessment performed with and without induced seismicity allows us to conclude that:

- The induced seismicity predicted by the different scenarios developed by Dynafrax predict only few and low earthquakes with magnitudes lower than 3.0.
- The increase in seismic hazard produced by the induced seismic source can be significant depending on the scenario chosen, even if the induced earthquakes are few. The reason is because the natural seismic hazard of the Groningen area is very low. Then, the addition of a new induced seismic source, even if this zone is not very active and can only produce low magnitudes, produces a non-negligible increase to the seismic hazard.
- The increase of seismic hazard (annual probability of exceedance of an acceleration threshold) is basically concentrated in the years of injection. When the injection stops, the seismicity returns to the natural (seismotectonic) situation. Considering long periods of time and diluting the increase of seismic hazard observed during the years of injection into a long period of time, the increase of seismic hazard is not significant.
- The increase in seismic hazard is not stationary and should be considered only for the next 1, 5, 10 or 30 years considered in the Dynafrax injection simulation. After

these years, the modelling shows that the induced seismicity tends to cease and should no longer be considered.
- The increase in seismic hazard affects mainly low accelerations (< 0.06 g).

From the seismic hazard point of view, some recommendations could be done:

- The best action would be to not inject any kind of fluid, independently of the rates and duration of the injection. The models used show that if the injection is zero, the induced seismicity tends also to zero.
- However, the seismicity shouldn't be the only criteria used to take a decision. For example, maybe the injection of fluids could allow a significant reduction of expected settlements and the benefits of the reduction of settlement could compensate the increment of seismic hazard.
- If finally, the injection is done, the preferred option would be the use of long periods of injection with small injection rates instead of short periods of injection using higher injection rate (the scenario 1 leads to annual exceedance rates lower than scenario 2, Figure 8.2 top).

10. References

AKKAR S. and BOMMER J. J. (2010). Empirical Equations for the Prediction of PGA, PGV, and Spectral Accelerations in Europe, the Mediterranean Region, and the Middle East, Seismological Research Letters, 81(2), 195-206.

AKKAR S., SANDIKKAYA M. A., and BOMMER J. J. (2014). Empirical Ground-Motion Models for Point- and Extended-Source Crustal Earthquake Scenarios in Europe and the Middle East, Bulletin of Earthquake Engineering, 12(1): 359 – 387

ARCADIS GERMANY GMBH & GEO-ENGINEERING.ORG GMBH (2018). Geological Desk Study Hollandse Kust (west) Wind Farm Zone. Project ID RVO.nl: WOZ2180087, 55 p.

ATKINSON, G. M. (2008). Ground-motion prediction equations for eastern North America from a referenced empirical approach: Implications for epistemic uncertainty, Bulletin of the Seismological Society of America, 98:3, 1304–1318

ATKINSON, G. A. (2015). Ground-Motion Prediction Equation for Small-to-Moderate Events at Short Hypocentral Distances, with Application to Induced-Seismicity Hazards. Bulletin of the Seismological Society of America. 105(2).

ATKINSON, G. A. and BOORE D. M. (2006). Earthquake Ground-Motion Prediction Equations for Eastern North America, Bulletin of the Seismological Society of America, Volume 96, No. 6, pages 2181-2205.

ATKINSON, G. M. and BOORE, D. M. (2011). Modifications to existing ground-motion prediction equations in light of new data, Bulletin of the Seismological Society of America, 101:3, 1121-1135

BASILI R., et al., (2013). The European Database of Seismogenic Faults (EDSF) compiled in the framework of the Project SHARE. http://diss.rm.ingv.it/share-edsf/

BINDI D., MASSA M., LUZI L., AMERI G., PACOR F., PUGLIA R. and P. AUGLIERA (2014), Pan-European ground motion prediction equations for the average horizontal component of PGA, PGV and 5 %-damped PSA at spectral periods of up to 3.0 s using the RESORCE dataset, Bulletin of Earthquake Engineering, 12(1), 391 – 340

BINDI D., COTTON F., KOTHA S.R., BOSSE C., STROMEYER D. and GRUENTHAL G. (2017) Application-driven ground motion prediction equation for seismic hazard assessments in non-cratonic moderate-seismicity areas", J. Seismology, 21(5), 1201 – 1218

BOMMER J. J., DOUGLAS J., SCHERBAUM F., COTTON F., BUNGUM H. and FAH D. (2010). On the selection of ground-motion prediction equations for seismic hazard analysis. Seismological Research Letters, Vol. 81, n° 5, p. 783-793BOSWORTH, W. (1989). Basin and range style tectonics in East Africa.

BOMMER J. J., DOST B., EDWARDS B., STAFFORD P. J., VAN ELK J., DOORNHOF D., NTINALEXIS M. (2016). Developing an Application-Specific Ground-Motion Model for Induced Seismicity. Bulletin of the Seismological Society of America; 106 (1): 158–173

BOMMER J. J., B. EDWARDS, P.P. KRUIVER, A. RODRIGUEZ-MAREK, P.J. STAFFORD, M. NTINALEXIS, E. RUIGROK, J. SPETZLER (2019). V6 Ground-Motion Model (GMM) for Induced Seismicity in the Groningen Field with Assurance Letter. NAM report.

BROUWER J.W.R. (2010). The meaning of Eurocode 8 and Induced Seismicity For Earthquake Engineering in the Netherlands. Fifth International Conference on Recent Advances in Geotechnical Earthquake Engineering and Soil Dynamics, May 24-29, San Diego, California.

BURKHARD M. & GRÜNTHAL G. (2009). "Seismic source zone characterization for the seismic hazard assessment project PEGASOS by the Expert Group 2 (EG1b)". Swiss Journal of Geosciences, Volume 102, Issue 1, p. 149–188.

CAMPBELL K.W. (2003) Prediction of Strong Ground Motion Using the Hybrid Empirical Method and Its Use in the Development of Ground Motion (Attenuation) Relations in Eastern North America" (Bulletin of the Seismological Society of America, Volume 93, Number 3, pages 1012-1033).

CAMPBELL K. W. and BOZORGNIA Y. (2008). NGA Ground Motion Model for the Geometric Mean Horizontal Component of PGA, PGV, PGD and 5 % Damped Linear Elastic Response Spectra for Periods Ranging from 0.01 to 10s" (Earthquake Spectra, Volume 24, Number 1, pages 139 - 171)

CAMPBELL K. W. and BOZORGNIA Y. (2014). NGA-West2 Ground Motion Model for the Average Horizontal Components of PGA, PGV, and 5 % Damped Linear Acceleration Response Spectra" (Earthquake Spectra, Volume 30, Number 3, pages 1087 - 1115).

CAUZZI C. and FACCIOLI E. (2008). Broadband (0.05 to 20 s) prediction of displacement response spectra based on worldwide digital records. Journal of Seismology, Vol. 12, n° 4, p. 453-475.

CAUZZI C., FACCIOLI E., VANINI M. et BIANCHINI A. (2015). Updated predictive equations for broadband (0.01 to 10 s) horizontal response spectra and peak ground motions, based on a global dataset of digital acceleration records. Bulletin of Earthquake Engineering, vol. 13, Issue 6, p. 1587-1612.

CHIOU B. S.-J. and Youngs R. R. (2008). An NGA Model for the Average Horizontal Component of Peak Ground Motion and Response Spectra" (Earthquake Spectra, Volume 24, No. 1, pages 173-215)

CORNELL, C. A. (1968). Engineering seismic risk analysis. Bulletin of the seismological society of America, 58(5), 1583-1606.

COTTON F., SCHERBAUM F., BOMMER J.J., BUNGUM H. (2006). Criteria for selecting and adjusting ground motion models for specific target regions: application to central Europe and rock sites. J. Seismol., 10, p. 137–156.

CROOK, Th. de, (1996), A seismic zoning map conforming to Eurocode 8, and practical earthquake parameter relations for the Netherlands, Geologie en Mijnbouw, 75, pp 11-18.

DELAVAUD, E., F. SCHERBAUM, N. KÜHN and T. ALLEN (2012). Testing the Global Applicability of Ground- Motion Prediction Equations for Active Shallow Crustal Regions. Bulletin of the Seismological Society of America. Vol. 102, n°2, p. 707-721

DERRAS B., BARD P. Y., COTTON F. (2014). Toward fully data driven ground-motion prediction models for Europe", Bulletin of Earthquake Engineering 12, 495-516

DOST, B., van Eck, T. and HAAK, H. (2004) Scaling of peak ground acceleration and peak ground velocity recorded in the Netherlands. Bollettino di Geofisica Teorica ed Applicata. 45(3), 153 – 168

DOUGLAS, J. (2010). Consistency of ground-motion predictions from the past four decades, Bulletin of Earthquake Engineering, 8, 1515-1526.

EC8 (2003). Eurocode 8: Design of structures for earthquake resistance - Part 1: General rules, seismic actions and rules for buildings. Ref. No. prEN 1998-1:2003 E.

FUGRO REPORT P904711/01 "Geotechnical Report Investigation Data Seafloor In Situ Test Locations Hollandse Kust (west) Wind Farm Zone Dutch Sector, North Sea"

GARDNER J.K. & KNOPOFF L. (1974). Is the sequence of earthquakes in Southern California, with aftershocks removed, Poissonian? Bulletin of the Seismological Society of America, 64, p. 1363–1367.

GIARDINI, D., GRUNTHAL, G., SHEDLOCK, K. M & ZHANG, P. (1999). The GSHAP global seismic hazard map. Ann. Geofisica 42: 1225-1230;

GIARDINI, D., J. WOESSNER, L. DANCIU (2014). Mapping Europe's Seismic Hazard. EOS, 95(29): p. 261-262.

GRÜNTHAL, G., BOSSE, C., SELLAMI, S., MAYER-ROSA, D. & GIARDINI, D. (1999). Compilation of the GSHAP regional seismic hazard for Europe, Africa and the Middle East. www.seismo.ethz.ch/static/GSHAP/index.html.

GRÜNTHAL, G., WAHLSTRÖM, R., STROMEYER, D. (2013): The SHARE European Earthquake Catalogue (SHEEC) for the time period 1900–2006 and its comparison to the European-Mediterranean Earthquake Catalogue (EMEC). - Journal of Seismology, 17, 4, 1339-1344.

GRÜNTHAL G., STROMEYER D., BOSSE C. (2017). The Data set of the earthquake model for the probabilistic seismic hazard assessment of Germany, version 2016. Report on supplementary material for the respective publication. Scientific technical report STR – Data; 17/05, PostDam

GRÜNTHAL, G., STROMEYER, D., BOSSE, C., COTTON, F. and BINDI, D. (2018). "The probabilistic seismic hazard assessment of Germany — version 2016, considering the range of epistemic uncertainties and aleatory variability ". Bulletin of Earthquake Engineering

HALE C., ABRAHAMSON N. and BOZORGNIA Y. (2018). Probabilistic Seismic Hazard Analysis Code Verification. PEER Report 2018/03

JOHNSTON, A.C., COPPERSMITH, K.J., KANTER, L.R. and CORNELL, C.A. (1994). "The Earthquakes of Stable Continental Regions". EPRI Technical Report TR-102261, 5 Volumes, Electric Power Research Institute, Palo Alto, California.

KNMI seismic catalogue. http://rdsa.knmi.nl/dataportal/.

LE DORTZ K., COMBES P., CARBON D. (2019). An alternative seismotectonic zonation for probabilistic and deterministic seismic hazard assessment for Metropolitan France. Submitted to the Bull. Soc. Geol. France.

ORDAZ, M., MARTINELLI, F., AGUILAR, A., ARBOLEDA, J., MELETTI, C., & D'AMICO, V. (2017). R-CRISIS. Program and platform for computing seismic hazard.

ORDAZ, M., MARTINELLI, F., AGUILAR, A., ARBOLEDA, J., MELETTI, C., & D'AMICO, V. (2018). R-CRISIS. Program and platform for computing seismic hazard.

ORDAZ, M. and SALGADO-GALVEZ M. A. (2019). R-CRISIS. Validation and Verification Document. ERN Technical Report. Mexico City, Mexico.

PAGANI M.; MONELLI D.; WEATHERILL G.; DANCIU L.; CROWLEY H.; SILVA V.; HENSHAW P.; BUTLER L.; NASTASI M.; PANZERI L.; SIMIONATO M.; VIGANO D. (2014). OpenQuake Engine: An Open Hazard (and Risk) Software for the Global Earthquake Model. Seismological Research Letters 85 (3): p. 692-702.

PAGANI M., J. GARCIA-PELAEZ, R. GEE, K. JOHNSON, V. POGGI, R. STYRON, G. WEATHERILL, M. SIMIONATO, D. VIGANÒ, L. DANCIU, D. MONELLI (2018). Global Earthquake Model (GEM) Seismic Hazard Map (version 2018.1 - December 2018).

STUCCHI M., et al. (2013). The share European earthquake catalogue (SHEEC) 1000–1899. Journal of seismology, volume 17, issue 2, p. 523–544.

TAVAKOLI B. and PEZESHK S. (2005) Empirical-Stochastic Ground-Motion Prediction for Eastern North America" (Bull. Seism. Soc. Am., Volume 95, No. 6, pages 283-2296)

TNO (2020a). Probabilistic Seismic Hazard and Risk Analysis in the TNO Model Chain Groningen, TNO 2020 R11052.

TNO (2020b). TNO Model Chain Groningen: Update and quick scan comparison of 2020 HRA model, TNO 2020 R11659.

TORO G. R., ABRAHAMSON N. A., SCHNEIDER J. F. (1997) Model of Strong Ground Motions from Earthquakes in Central and Eastern North America: Best Estimates and Uncertainties. (Seismological Research Letters, Volume 68, Number 1)

TORO, G.R. (2002). Modification of the Toro et al. (1997) attenuation equations for large magnitudes and short distances, Technical Report, Risk Engineering.

VERBEECK K., VANNESTE K., CAMELBEECK T. (2009). “Seismotectonic zones for probabilistic seismic-hazard assessment in Belgium”. ONDRAF/NIRAS report, Belgium agency for radioactive waste and enriched fissile materials. NIROND-TR Report 2008-31E. 61 pp.

WEICHERT, D.H. (1980). Estimation of the earthquake recurrence parameters for unequal observational periods for different magnitudes, Bulletin of the Seismological Society of America, 70, p. 1337-134

WOESSNER, J., DANCIU, L., GIARDINI, D. and the SHARE consortium. (2015). “The 2013 European Seismic Hazard Model: key components and results”. *Bulletin of Earthquake Engineering*.

YENIER E. and ATKINSON G. M. (2015). Regionally Adjustable Generic Ground-Motion Prediction Equation to Central and Eastern North America" BSSA, vol 105

ZHAO, J.X., ZHANG, J., ASANO, A., OHNO, Y., OOUCHI, T., TAKAHASHI, T., OGAWA, H., IRIKURA, K., THIO, H.K., SOMERVILLE, P.G., FUKUSHIMA, Y., FUKUSHIMA, Y. (2006) Attenuation relations of strong ground motion in Japan using site classification based on predominant period, Bulletin of the Seismological Society of America, 96:3, 898–913